We thank the referees for their reviews and their suggestions which helped to clarify the manuscript. We addressed the comments in point-by-point replies and inserted the according text changes into the revised manuscript.

In this document we duplicated the referees comments followed by individual responses, and attached a marked-upversion (latexdiff) of the manuscript.

Figure 2 and Fig.3 have been adapted for further clarification. Figure 7 has been reworked using LAI instead of GPP.

Thank you for your review and your comments that help to clarify the manuscript. Below we duplicate your comments (**bold**) and respond to them point-by-point (*italics*) followed by modifications that will be adopted in the revised manuscript.

1. The text raises two important expectations that were not fulfilled in the results. First is the issue of land-atmosphere interactions. I would argue that it is conventional to think of land-atmosphere interactions in terms of energy and water budgets, and indeed some authors (e.g., Santanello Jr et al. 2018) define land-atmosphere interactions exclusively in terms of energy and water budgets. Yet the current manuscript contains no results related to energy and water budgets. Personally, I think that such results would be an interesting addition to the paper. Without such an addition, I think the authors need to change the text to more specifically refer to carbon fluxes and budgets.

Thank you for pointing this out. We adapted the text in several places to not raise the expectation of presenting results related to energy and water budgets (just for variables influencing energy and water budgets, in particular LAI). We further tested the response of evapotranspiration (ET) and we attached a figure showing the change in NRMSE for ET to the review responses (Fig. R1). Figure R1 shows that the shape of the change in NRMSE is comparable to that for LAI, however, the magnitude is smaller. We thus feel that the ET plot would not add much information and decided not to show the figure in the manuscript.

Examples of sentences changed in the text: The second and third sentence of the abstract now state

Forest age-structures in turn influence ~~biophysical and biogeochemical interactions of the vegetation with the atmosphere~~ key land surface processes, such as photosynthesis and thus the carbon cycle. Yet, many dynamic global vegetation models (DGVMs), including those used as land surface models (LSMs) in Earth system models (ESMs), do not account for subgrid forest age structures, despite being used to investigate land-use effects on the global carbon budget or simulating ~~land–atmosphere interactions~~ biogeochemical responses to climate change.

The second sentence of the summary and outlook section now states:

JSBACH4–FF allows ~~land–atmosphere interactions~~ key land surface processes to be simulated in dependence of forest age and, simultaneously, to trace the exact forest age, ~~enabling the~~ which is a precondition for any implementation of age-based forest management schemes in JSBACH4–FF.

Second is the issue of forest management. The authors repeatedly state (see P11,L10-11 for one example) that an advantage of the model is in simulating different forest management scenarios. However, this is not exploited in the paper (I know that the forest management scenarios in Fig. 7 are different, but so is the climate, so one cannot isolate the effect of the management scenario). Why not illustrate the power of the new modelling approach by running different forest management scenarios for a single grid cell?

The main purpose of the paper was the description of the implementation of forest age-classes in JSBACH4 and the presentation of the applied new approach for this introduction of forest age-classes. The possibility to implement different forest management scenarios is one important motivation for this model development, but neither the only motivation, nor a focus of our paper and we consider running the model for several more forest management scenarios beyond the scope of this study. In order to not suggest the focus of our study is studying effects of various forest management scenarios we adapted the text in several places. However, we would like to note that technically we in fact do compare two different forest management scenarios, namely the average harvest in the PFT simulation and the harvest of the oldest forest area in the age-class simulations (under the same climate).

Examples for adapted text passages – line 8-9 first page:

~~Our scheme combines~~ The first being a computationally efficient age-dependent simulation of all relevant processes, such as photosynthesis and respiration, ~~without loosing the information about~~ using a restricted number of age-classes. The second being the tracking of the exact forest age, which is a prerequisite for ~~the~~ any implementation of age-based forest management.

First sentence of the results and discussions section:

Having forest age-classes in JSBACH4–FF facilitates a finer discretisation in each grid-cell and ~~enables the~~ is a precondition for any implementation of age-based forest management.

Additionally we inserted a statement on the two applied forest management schemes in the Section on harvest maps (now 2.3.4):

In different simulation types – with or without age-classes – the same harvest maps were used, but different forest management schemes were applied. In simulations with age-classes, a clear-cut according to the fractions in the harvest map was taken from the oldest age-class. In the simulation without age-classes, the PFT simulation, we used the same harvest fractions as in the simulations with age-classes, but harvest was applied as done in JSBACH3 (Reick et al., 2013), i.e. by diluting the wood carbon of the harvested PFT tile.

2. Some of the methods were not adequately justified. First, I am concerned that the initial condition is unrealistic. Why did simulations begin in 1860 from bare ground rather than from a spin-up? Of course, the 1860 initial condition would more realistically be represented by many forested areas.

Thanks for pointing this out, we have now added our reasoning to start from scratch in 1860:

Simulations started in 1860 from scratch, i.e. with empty vegetation carbon stocks, and were run up to 2010. Empty carbon stocks are a simplification used in the absence of global knowledge on the state of the forest in 1860, but have no influence on our results, since in simulations with JSBACH4 (4.20p7) LAI, GPP and AGB only depend on the age since the last clearing event, not on the history before that. The starting date of 1860 was chosen such that it covers at least one full cycle of regrowth, as the oldest age resolved in the simulations matches that of the observation-based data (Poulter et al., 2018).

Note that the used JSBACH version has no influence of soil carbon and nutrient state on vegetation growth, which could be influenced by the history prior to the last clearing event,.

Second, I could not determine from the paper how one goes from the 2010 age-class distribution to time-dependent (1860-2010) harvest rates. This procedure should be described.

We did outline the derivation of the annual harvest maps in 2.4.3. (now 2.3.4), and described the procedure in detail in the supplementary material S2.For the procedure deriving the harvest rates we politely point the referee to the listing in S2.

Third, it seems like there is an inconsistency between the definition of the model's PFTs (tropical evergreen and deciduous, extratropical evergreen and deciduous) and the Poulter et al. PFTs (broadleaf evergreen and deciduous, needleleaf evergreen and deciduous). What is the correspondence?

We added the mapping formula to 2.4.3 were we previously only stated that the Poulter et al. (2018) PFTs were mapped to JSBACH's PFT cover fractions.

Part of the edited text in 2.4.3:

The map by Poulter et al. (2018) provides a grid with 0.5 ◦ resolution of the global forest age distribution of ~~4 forest PFTs(needleleaf evergreen and deciduous~~four forest PFTs: needleleaf evergreen (NE) and needleleaf deciduous (DE), as well as broadleaf evergreen ~~and deciduous) on a grid with 0.5resolution~~ (BE) and broadleaf deciduous (BD). The map uses a discretisation into 15 age-classes, covering 10 years each, with the last class containing all area with an age >140 years. In a pre-processing step, the map was remapped to T63 using the conservative remapping operator of the CDOs. Subsequently, the ~~PFTs from the map were scaled to~~area sums of the two evergreen and the area sums of the two deciduous PFTs from Poulter et al. (2018) were used to derive the age-class maps for JSBACH's ~~PFT cover fractions. From these scaled~~evergreen and deciduous PFTs, respectively, following Eq. 6

3. The comparison to observations can be made more substantial. RMSE is a helpful statistic, but I wonder what is being missed by only considering this statistic. For example, I wonder what can be learned from Taylor diagrams? I am certainly not asking that the paper include Taylor diagrams for every variable, but rather such diagrams could be analyzed in a preliminary analysis and the most exciting ones presented in the paper or supporting information.

Following this suggestion we performed an analysis using Taylor diagrams comparing the PFT simulation, i.e. the simulation without age-classes with the IAS11 simulation, i.e. the age-class set up used in the more detailed comparison in the manuscript. We included the Taylor diagrams in the supplementary and added a note in the methods section. However, since we found that the Taylor diagrams do not allow new, important conclusions to be drawn beyond the NRMSE comparison, we did not include further analysis of the Taylor plots in the results section.

Text added to Section 2.2 (previously 2.2)

In addition, we created Taylor diagrams for each variable, season and region (see Figures S5.5–S5.11 in the supplementary).

4. There are some problems with the interpretation of the results. First, I think it misses the point to repeatedly state that the new model is better. Rather, the fundamental result is that new model tends to reduce GPP and LAI relative to the old model. The new model is better because the old model was biased high. If the old model had been unbiased, then the new model would have been biased low. Alternatively, suppose that there is another modeling group excited by this study, and that that modeling group has a model that is biased low. Then implementation of this scheme would probably make that model worse.

We agree that our implementation of age-classes in a model with a low bias would probably make such a model even worse and adapted the manuscript to stress that introducing the age-classes in a model which is biased low would lead to an increase in the comparison error. We also agree that results closer to observations could just be a consequence of compensating for a high bias (for whatever reason that high bias may have existed) in the old model and now distinguish between model improvement in terms of quantitative results (which could be disputed) and model improvement in terms of inclusion of processes known to exist in reality (in the latter respect the new model is clearly "better"). Nevertheless, we would like to point out that spatially explicit comparisons of the results from the PFT simulation and observation-based data ("OBS-PFT" in Figs. S4.2–S4.4, column 2) indicate several areas of underestimation (red) and of overestimation (blue) for all variables, thus the old model was not merely biased high.

In addition, we have tried to understand if the high bias in the old model is due to not including age-classes or due to other processes. We found that indeed part of the high bias stems from missing an adequate representation of regrowth: we attached a figure showing the change in model bias per mean

age to the review responses (Fig.R2). Figure R2 shows that the change in model bias decreases with forest age, indicating that the error reduction happens where the old model was biased high due to not considering forest age.

In the results and discussions section looking at the benefit of having age-classes (3.2) we inserted the following summary and caveat:

In summary, simulations using age-classes led to a decrease in the simulated GPP, LAI and AGB values due to their non-linear increase with a saturation for older ages. This caused a decrease in the $NRMSE_{Max-Min}$ in areas where the PFT simulation was biased high and an increase in the $NRMSE_{Max-Min}$ in areas where the PFT simulation was biased low. Thus, if such a forest age-structure would be implemented in a DGVM being predominately biased low, the difference to the observation-based data could increase.

Second, I think that more care needs to be taken in the interpretation of Figure 6. While the curves in panels a-c are decreasing, the authors do not quantitatively support their assertion that the curves are decreasing exponentially (and not, say, quadratically). Exponential fits should be done and the quality of the fits should be analyzed if the authors want to assert that the declines are exponential. Related to this, the assertion that there is "no offset" in panel d is unsupported. A linear fit should be done, and analysis of the residuals would inform whether there is an offset.

Concerning the shape of the curves in panels a-c: We eliminate statements about the shape of the curve, since this is not relevant for our conclusions. The second last sentence of the abstract, for example, now states:

The comparisons show ~~differences exponentially decreasing with the~~decreasing differences and increasing computation costs with an increasing number of distinguished age-classes~~ and linearly increasing computation costs~~.

Concerning computing time (panel d): The pre-last paragraph of the Evaluation section (3.1) now reads:

Comparisons of required CPU times show a ~~linear~~ near-linear increase with an increased number of age-classes (Fig. 6d) and neither a difference between the two age distribution schemes, nor ~~an~~a striking offset as compared to the PFT simulation. ~~This behaviour~~A near-linear increase with an increased number of age-classes was expected, since the processes requiring most of the computing time, such as the calculation of photosynthesis, carbon allocation and respiration, are conducted on the age-classes. The absence of ~~an~~a striking offset comparing the PFT simulation with the age-class simulations indicates that the introduced organisational overhead on the PFT level in simulations with age-classes~~ is not substantial~~, i.e. tracing of the exact forest age and redistributions of area fractions and other state variables among tiles, is not dominating the computation times.

5. In Section 3.3, note that much of the discussion is also relevant to cohort-based models (or at least the ED family). The ED approach involves discretization of a partial differential equation (equation 5 in Moorcroft et al. 2001), and thus there are again questions of the optimal number of age bins, whether the bins should be of different or equal sizes, and criteria for merging.

Thank you for this comment.

Technical corrections

P1, L8: do you mean "simulation" rather than "implementation"? This paper, of course, deals with the simulations rather than actual implementations of forest management.

We actually meant implementation. We split and rephrased the sentence, now stating:

In this paper we present a new scheme to introduce forest age-classes in hierarchical tile-based DGVMs combining benefits of recently applied approaches. ~~Our scheme combines~~ The first being a computationally efficient age-dependent simulation of all relevant processes, such as photosynthesis and respiration, ~~without loosing the information about~~ using a restricted number of age-classes. The second being the tracking of the exact forest age, which is a prerequisite for ~~the~~ any implementation of age-based forest management.

P1, L9: not clear what "hierarchy" is being referred to here

Thank you. We edited this sentence.

This combination is achieved by using the tile-hierarchy to track the area fraction for each age on an aggregated plant functional type level, whilst simulating the relevant processes for a set of age-classes.

P2, L11: replace "extend" with "extent"

Changed accordingly.

P2, L13-16: there are a couple of sentences where a plural verb "are" is used with a singular subject ("one example")

Changed accordingly.

P3, L5: this sentence seems to have missing words or typos

Thank you, we corrected "extent" to "expand".

P3, L6: I am comfortable with the idea that this is a frequently applied approach, but do you have evidence that this is the "most frequently" applied approach?

We edited the sentence and now state that it is the more commonly used (of the two recently developed approaches that we present, based on the number of references that we found and list using one or the other approach):

To ~~extent~~expand tile-based DGVMs to represent subgrid forest age structures, two approaches have recently been developed. The ~~most~~more frequently applied approach has been to increase the number of tiles in such a way that a certain number of age-classes or structurally similar stands can be distinguished.

P3, L30: Perhaps instead of "In this paper we try to", use "The objective of this paper is to"

We edited the sentence, it now states:

In this paper we ~~try to~~bridge the two approaches for extending tile-based DGVMs to represent subgrid forest age in the sense that we present a way to trace the actual age of the forests in a grid-cell despite following the first approach using a restricted number of additional tiles and thus required merges.

P7, L4: Note that "data" is plural. Hence, "these data".

Changed to "datasets".

Throughout: My sense is that the word "exemplary" is not being used appropriately in the text. Exemplary denotes a particularly good example, whereas I think the authors are oftentimes just referring to an example of the typical sort.

We replaced the three occurrences of exemplary in the manuscript.

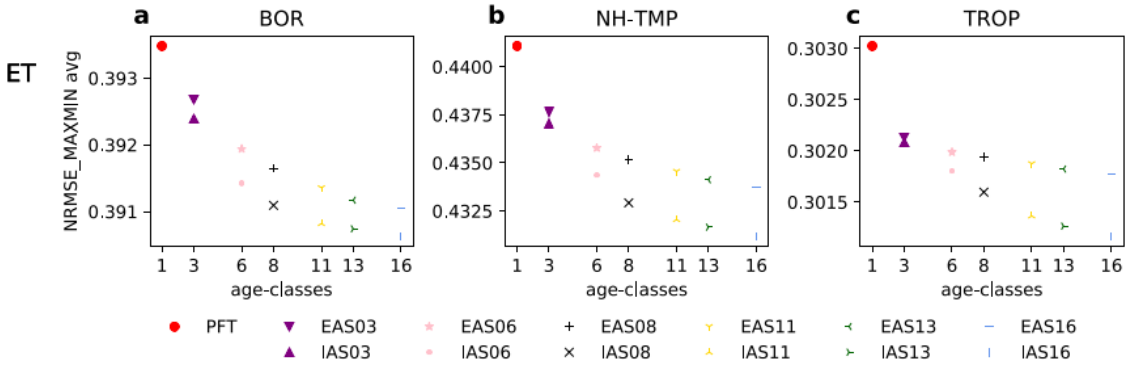

Figure R1: Change in $NRMSE_{Max-Min}$ when comparing simulated evapotranspiration (ET) of simulations using an increasing number of age-classes to observation based ET data (GLEAM V2A – Miralles et al., 2011). As in the comparison for GPP, LAI and AGB (Supplementary figure S3.1) averaging has been conducted giving equal weights to each of the four seasons.

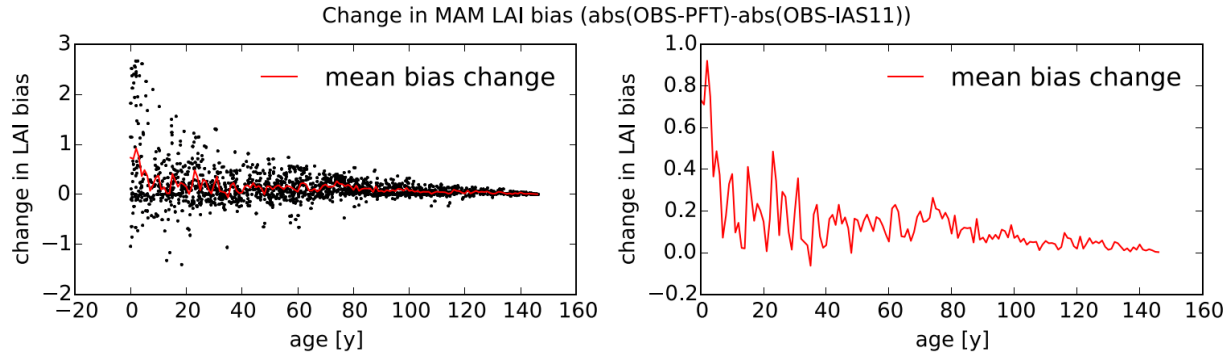

Figure R2: Change in the difference of the differences of simulated and observed MAM LAI using the PFT and the IAS11 simulation. Dots mark differences in single grid-points at grid-point mean ages, the red line marks the mean change of all dots for each mean-age (rounded to integer years). Note the difference in the y-axis of the two panels.

References

Miralles, D. G., et al. "Magnitude and variability of land evaporation and its components at the global scale." (2011).

Thank you for your review and the suggestions that help to clarify the manuscript. We have duplicated your comments (**bold**) below, each followed by a point-by-point response (*italics*) including the modifications that will be adopted in the revised manuscript.

(1)The description of model "development" part needs to be strengthened. In general, the authors failed to highlight their technical advances or difficulties in contrast to the original model version (or the complexity the development that's achieved) to allow reviewer to appreciate their work. I agree this hierarchical structure in JSBACH is novel and it seems to facilitate the management of which processes to be executed on which level to save computation time (as the authors claimed but is not actually shown). Is this feature out of the development by the authors in this work? Otherwise it seems that the authors just made use of this existing model feature and did some simple configuration changes (mainly the number of age classes and their distribution over age) and they claimed this as a new "development". For "development", I would understand as substantive new features in the model, or improvement in parameterization, or new method for model calibration etc. It seems the only paragraph that's fully dedicated to the "development", or the description of the author's new work is the first paragraph in Section 2.3. All other material in the "Methods" section is devoted to introducing JSBACH model structure (2.1), or existing hierarchical model feature (2.2) or simulation set-up (2.4). With this it's hard to appreciate what's really achieved in this paper in terms of "model development". The whole paper more sounds like testing a configuration of the model in terms of age class and performing some sanity check in GPP, LAI and AGB. That's how I reach the feeling of an interval technical report.

Thank you for this important comment. We rewrote large parts of Section 2.1 and the former Section 2.3 (now 2.2) and adapted Fig.2 and Fig.3 to better explain the newly developed scheme and to better emphasise new model developments. The tile hierarchy did indeed already exist, however, as a purely infrastructural piece of code. For each of the introduced process this infrastructure had to be extended. In particular, we newly introduced the age vector to track the age, and the processes managing the age-classes. These processes were either newly implemented (ageing and harvest) or had to be advanced (disturbances). An additional major technical advancement was to address the new necessity to introduce shifts of area fractions from one AC to another, as well as resulting shifts of forest carbon and the re-determination of other affected state variables. We now also describe these new infrastructural developments.

(2)There is great confusion in this hierarchical model structure and the advantages that the authors claimed to have. If this overall, sharing model "overhead" can really save computation time, we would expect a non-linear relationship in Fig. 6d ? A decreasing amount of extra time used for each unit increase in number of age class should be expected. From this, I don't see the author's claim that such a feature that different age classes share some common "overhead" process to be computationally efficient as being proved.

Thank you for pointing this out. We assume that different concepts got mixed up, being (1) what we called the "organisational overhead", (2) savings of computation time by only introducing a restricted number of age classes, and (3) the potential to save computation time by simulating processes on different levels of the tile-hierarchy. When rewriting Section 2.1 and the former Section 2.3 (now 2.2), as well as upon adding to Fig.2 and Fig.3, we attempted to resolve this confusion. We particularly removed statements targeting point (3) listed above since these are not directly connected to the developments presented in our paper. For clarification: we used "organisational overhead" to refer to the additional computation time required for bookkeeping of the exact forest age and managing merges of fractions of different age-classes.

In addition to rewriting Sections 2.1-2.3 (now 2.1 and 2.2) we explain what we term the "organisational overhead" on its first occurrence in Section 3.1, stating:

The absence of ~~an~~a striking offset comparing the PFT simulation with the age-class simulations indicates that the introduced organisational overhead on the PFT level in simulations with age-classes ~~is not substantial~~, i.e. tracing of the exact forest age and redistributions of area fractions and other state variables among tiles, is not dominating the computation times.

(3)Relate to the above point. The authors mentioned throughout the paper the importance of biophysical feedbacks of forest management but nothing of this aspect is shown in the paper. Instead, there is little description on how such processes are simulated in the age-class model structure. The only text I found that gives such similar description seems to be lines 10-13 in Section 2.2 but this is quite vague. The readers are left wandering in what processes belong to "overhead" and which are age-class specific ? For example, how the processes like albedo, energy balance, soil water processes, carbon allocation are simulated ?

When rewriting Section 2.1 and the former Section 2.3 (now 2.2) we attempted to also resolve this point changing the text to make more explicit (1) which processes already were present in the basis version of JSBACH4 and which have been implemented in the course of this study and (2) on which level of the hierarchy the different processes are executed. Regarding raised expectations concerning biogeophysical feedbacks (which was also commented by reviewer 1, comment 1) we adapted the text in several places to not raise the expectation of presenting results related to energy and water budgets (just for variables influencing energy and water budgets, in particular LAI). We further tested the response of evapotranspiration (ET) and we attached a figure showing the change in NRMSE for ET to the responses to reviewer 1 (Fig. R1). Figure R1 shows that the shape of the change in NRMSE is comparable to that for LAI, however, the magnitude is smaller. We thus feel that the ET plot would not add much information and decided not to show the figure in the manuscript.

Which of these processes are "overhead" and how flexible they are in terms of being simulated on different levels ? These are critical for the age-class feature to really reflect forest management impacts but are unfortunately little described.

We made several text changes, particularly in the former Section 2.3 (now 2.2), as well as additions to Fig. 2 and Fig. 3, to make more explicit which processes and state variables are located on which level (please also see the response to point 1). Regarding the term "overhead", please also refer to response 2.

(4)The essence of the new age-class feature is to yield lower estimate of LAI, GPP and AGB than the old version. Comparing the overall agreement between the old and new feature with observation is nice but not the most convincing way from my point of view, because the old version can always be adjusted/parameterized to agree with the observation and if this is the case, the new version would show a prevalent low bias.

We agree that the new model version does show a better performance where the old model version was biased high, particularly in several of the regions having young forests. Nevertheless, we would like to point out that the improved model performance is related to not considering forest age (see Fig.R2 in the responses to reviewer 1). Furthermore, we would like to point out that spatially explicit comparisons of the results from the PFT simulation and observation-based data ("OBS-PFT" in Figs. S4.2–S4.4, column 2) indicate several areas of underestimation (red) and of overestimation (blue) for all variables, thus the old model was not merely biased high. Tuning the old version could potentially result in a lower high bias in regions where the forest is young, but this will result in a low bias in regions where the same PFT is mature. So, tuning is not an alternative to including age classes. In order to raise awareness of the general direction of biases (which was also commented on by reviewer 1, comment 4) we inserted the

following summary and caveat in the results and discussions section looking at the benefit of having age-classes (3.2):

In summary, simulations using age-classes led to a decrease in the simulated GPP, LAI and AGB values due to their non-linear increase with a saturation for older ages. This caused a decrease in the $NRMSE_{Max-Min}$ in areas where the PFT simulation was biased high and an increase in the $NRMSE_{Max-Min}$ in areas where the PFT simulation was biased low. Thus, if such a forest age-structure would be implemented in a DGVM being predominately biased low, the difference to the observation-based data could increase.

What would be nice is to show whether the model improvement is systematically related to the forest age. For example, is the bias or error reduction more pronounced in regions where young forests dominate? What the processes driving such a decrease in simulated LAI, GPP and AGB and how does this relates to the "ageing" process in the model? The author mentioned several times of this "ageing" process but what is it and how does it impact the simulation of these variables? Are examples of new model behaviour related to age-class development is necessary to understand this? Another way to show the influence of this new development is to show its impact on estimated global fluxes, such as land use change emissions as the authors described in the introduction.

For the relation of the improvement in model performance and forest age please refer to Fig. R2 in the responses to reviewer 1. Regarding the simulation of LAI, GPP and AGB: their relation to the "ageing process" stems from LAI, GPP and AGB being simulated separately for each age-class. Due to the non-linear relationship of GPP, LAI and AGB with forest age (Fig.7 of the manuscript) simulations of a mixed aged forest will result in higher values in a mean age forest simulation (PFT) than in a simulation resolving different age-classes and thus leading to independent simulations of LAI, GPP and AGB on tiles representing different forest ages. Regarding the explanation of the ageing process: we added a more detailed description of the process in 2.2:

Ageing The ~~ageing of forests happens annuallyand affects the oldest year in each AC~~newly implemented process of forest "ageing" happens annually: upon ageing each tracked forest fraction gets one year older. Yet, a shift from one age-class to the next age-class only happens for the area of the oldest age ($maxA_{K-1}$-*1*) of an age-class AC_{K-1}, i.e. only the forest area which upon getting one year older ~~the fraction of forests having age $maxA_{M-1}$~~exceeds the upper age bound $maxA_{K-1}$ of the AC_{K-1} needs to be shifted into AC_K. Thanks to the tracking of the age in the *fractPerAge* vector, the exact area fraction with age $maxA_{K-1}$-*1* ~~will shift from AC_{M-1} into AC_M~~is known.

Some minor and editorial comments:

P 3 line 5 : "to extent" -> extend

Changed accordingly.

P4 line 12: "be able to" could be removed.

The sentence has been adapted (see response to the next comment).

P4 line 11: "a dependency of the maximum leaf area index (LAI) on the available leaf carbon ", what do you mean by "available leaf carbon", does it mean existing leaf biomass or NPP that's allocated to leaf? I would think it is rather natural and reasonable that maximum LAI being limited by leaf biomass? How do this feature relate to the age class development ? Is this feature already satisfying for age class structure, or not ?

We agree with the referee that it is natural and reasonable that the maximum LAI, i.e. the LAI that can maximally be reached at the peak of a season, is limited by leaf biomass. However, this is not the case in the standard JSBACH3 (Mauritsen et al., 2019) version and therefore also not in the standard JSBACH4 version. In JSBACH3, the maximum LAI is a PFT-dependent constant, which is why we implemented this dependency in an independent study (Naudts et al., in prep.). We now explicitly stress that this was not the case in JSBACH3 and that it is a precondition for the introduction of our age-classes. We rewrote this part of Section 2.1 now stating:

As an important amendment to the current version (4.20p7) ~~used as basis in this paper has been amended by a dependency of the~~, we ported a new JSBACH3 development, which we implemented in a recent independent study (Naudts et al., in prep.): While previous JSBACH3 versions assumed a PFT-dependent but constant maximum leaf area index (LAI), that is the LAI value that can maximally be reached at the peak of a season, Naudts et al. (in prep.) introduced a dependency of the maximum LAI on the available leaf ~~carbon, which only recently has been implemented in JSBACH3 (Naudts et al., in prep.)~~biomass. Such a dependency is a prerequisite for simulating forest re-growth and thus for the introduction of age-classes.

P6 line 2: is the "git" feature relevant here, it has been mentioned several times including the in the title.

We prefer to keep this information for reproducibility reasons.

P 6 line 4: the upper-bound of what ?

Thank you for pointing this out. We edited this (and other) sentences. This sentence now states:

In addition, ~~the upper-bound of each~~a to be pre-defined upper age bound per age-class AC_M ~~($maxA_M$)~~$_K$ ($maxA_K$) as well as ~~the~~a total maximum age (maxAge) ~~need to be pre-defined~~were introduced.

P 6 line 20: "initiated" can be removed.

This sentence changed upon rewriting of Section 2.3 (now 2.2).

P 6 line 21-22: "which are directed and scheduled on the PFT level but exerted on the ACs ". I don't get the meaning, could it be explained in an easier way ?

This sentence changed upon rewriting of Section 2.3 (now 2.2).

P 7 line 4: Some brief introduction on GPP and LAI data is needed. A critical issue here: as far as I understand Tramontana et al. 2016 GPP data does not consider forest age and it's questionable to use this as a product to evaluate a model with age effect because the age is the key point here. A recent paper by Besnard et al. ERL (https://doi.org/10.1088/1748-9326/aaeaeb) tried to address this but I don't know whether they have GPP product. Likewise, is the LAI data pure satellite observation?

Thank you for pointing this out. We now briefly introduce GPP and LAI in Section 2.3.1. Furthermore, we added some caveats regarding the observation-based data in Section 3.2. Additionally, we redid Fig.7 in the text using LAI instead of GPP.

Brief introduction in Section 2.2.1 (former 2.3.1):

We used ~~GPP and LAI data for the year~~2010 ~~as derived in Tramontana et al. (2016). This data already had~~MODIS LAI (Myneni et al., 2002) and GPP data obtained from machine learning methods trained on flux-tower measurements (Tramontana et al., 2016).

Added sentences in Section 3.2:

In this context, caveats regarding the observation-based data themselves need to be raised. A known caveat regarding MODIS LAI data is the problem of reflectance saturation in dense canopies making the reflectance insensitive to changes in LAI (Myneni et al., 2002). This problem, which is particularly relevant to the tropical region, could lead to a general high bias of the model compared to the observation-based data. However, since this problem is more typical for denser old grown forests, this high bias would also occur in the simulations with age-classes. Regarding the GPP data from Tramontana et al. (2016), a recent study by Besnard et al. (2018) criticised that the applied empirical upscaling techniques do not directly consider forest age, making it unclear how well they can capture age-related dynamics. In their study, Besnard et al. (2018) advocate the development of alternative global datasets considering forest age as a predictor.

P 8 line 24 : "to be harvested fraction" -> to-be-harvested-fraction ? A noun form should be here but please check.

The sentence was superfluous and has been deleted.

Figure 2: what's the "UML" ?

Now spelled out (Unified Modeling Language).

Figure 3: AC M , I would use AC i , which distinguishes clearly with AC N ,i.e., the former refers to a common AC, while the latter refer to the old-growth AC.

Thank you very much for this suggestion. We updated the figure accordingly (for better readability we used K instead of I). We also replaced all occurrences of AC M in the text by AC K.

Figure 5: Label for vertical axis not consistent with others. Can you use more expressive label, for example, "Normalized RMSE?".

Fig.5 shows the $NRMSE_{Max-Min}$ for each variable, region and season. Fig.6 and Fig. S3.1 show averages over the seasons or the seasons and the regions, respectively. Therefore, the y-axis of these figures are labeled differently. We added "normalised root mean squared error" to the figure captions.

Equation (2): I would write simply N-1 for the denominator...

In the former EQ.2 (now EQ.4) the denominator should contain the sum of i's (i.e. for N=5: 1+2+3+4 = 10). However, there had been a mistake in the equation (the sum over the i's started with i), which we now corrected.

P12 line 1: "as also discussed" -> as is also discussed

Changed accordingly.

Figure 7, caption: "Stars mark the JJA GPP per age-class", please indicate this is for simulated data.

Changed accordingly.

Could you somehow simply the caption ? It's rather long and almost deters reading.

We tried to shorten the caption, but it still remains long as we prefer to include all the information necessary to read the figure. The caption now reads:

Example grid-points comparing 2001-2010 mean spring leaf area index (MAM LAI) from simulation without (PFT) and with age-classes (IAS11) to observation-based data. The map in the center shows the difference of differences between the observation-based data and the simulations (abs(OBS-PFT)-abs(OBS-IAS11)), i.e. it shows where the results from the simulation with age-classes (IAS11) deviate less (blue) or more (red) from the observation-based data than the PFT simulation results (see also Figs. S4.2-S4.4, column 4). Dashed lines in the map mark the three selected regions (see Table 2). The plots (a-g) show the LAI of selected PFTs (ETD: extratropical deciduous; ETE: extratropical evergreen; TD: tropical deciduous; TE: tropical evergreen) as well as their according area fractions per age-class and per year at the labelled grid-points. Center latitude, longitude and grid-cell cover fraction (cf) of the depicted PFT are indicated. The x-axis reflects the age from 0-151 (purple) with the age-classes (black) indicated at the age centres. The two right y-axes represent the bars: depict are the 2010 area fractions relative to the area of the depicted PFT. Blue bars are per age-class (black y-axes) and depict the fraction of each age-class (i.e. one bar per age-class); the yellow framed purple bars depict the fraction of each age (i.e. one bar per year). The left y-axis depicts the LAI. Stars mark the simulated LAI per age-class, and the lines the LAI of the depicted PFT – blue dashed line: IAS11 simulation, black line: PFT simulation, green line: 2010 value from the observation-based data. Note: 1. The age-class LAI is only depicted for age-classes having non-zero fractional cover over the whole timespan 2001-2010 (this is not the case for the age-classes 9 and 10 in panel c, f and g). 2. Age and age-class fractions of classes 2-8 in panel g are very small and therefore not visible above the x-axis. 3. Since we did not apply any harvest in the final simulation year 2010, the first year and accordingly the youngest age-class are always empty.

Accounting for forest age in the tile-based dynamic global vegetation model JSBACH4 (4.20p7; git feature/forests) – a land surface model for the ICON-ESM

Julia E. M. S. Nabel[1], Kim Naudts[1,a], and Julia Pongratz[1,b]

[1]Max Planck Institute for Meteorology, 20146 Hamburg, Germany
[a]now at: Department of Earth Sciences, VU University Amsterdam, The Netherlands
[b]now at: Ludwig-Maximilians-Universität München, Munich, Germany

Correspondence: J. E. M. S. Nabel (julia.nabel@mpimet.mpg.de, jemsnabel@gmail.com)

Abstract. Natural and anthropogenic disturbances, in particular forest management, affect forest age-structures all around the globe. Forest age-structures in turn influence ~~biophysical and biogeochemical interactions of the vegetation with the atmosphere~~key land surface processes, such as photosynthesis and thus the carbon cycle. Yet, many dynamic global vegetation models (DGVMs), including those used as land surface models (LSMs) in Earth system models (ESMs), do not account for subgrid forest age structures, despite being used to investigate land-use effects on the global carbon budget or simulating ~~land–atmosphere interactions~~biogeochemical responses to climate change. In this paper we present a new scheme to introduce forest age-classes in hierarchical tile-based DGVMs combining benefits of recently applied approaches. ~~Our scheme combines~~ The first being a computationally efficient age-dependent simulation of all relevant processes, such as photosynthesis and respiration, ~~without loosing the information about~~ using a restricted number of age-classes. The second being the tracking of the exact forest age, which is a prerequisite for ~~the~~ any implementation of age-based forest management. This combination is achieved by using the ~~hierarchy~~ tile-hierarchy to track the area fraction for each age on an aggregated plant functional type level, whilst simulating the relevant processes for a set of age-classes. We describe how we implemented this scheme in JSBACH4, the LSM of the ICON-ESM. Subsequently, we compare simulation output against global observation-based products for gross primary production, leaf area index and above-ground biomass to assess the ability of simulations with and without age-classes to reproduce the annual cycle and large-scale spatial patterns of these variables. The comparisons show ~~differences exponentially decreasing with the~~ decreasing differences and increasing computation costs with an increasing number of distinguished age-classes~~and linearly increasing computation costs~~. The results demonstrate the benefit of the introduction of age-classes, with the optimal number of age-classes being a compromise between computation costs and ~~accuracy~~error reduction.

1 Introduction

Land use, particularly forest management, substantially influences the age structure of global forests (Pan et al., 2011; Erb et al., 2017). More than 19 M km^2 of forest area, i.e. about 15% of global ice-free land, are under some kind of management

(Luyssaert et al., 2014), with 65% being under regular harvest schemes and another 7% being intensive plantations (Erb et al., 2017). Often, management practices make use of rotation cycles, as common in shifting-cultivation (Boserup, 1966) or even-aged forest management strategies that historically were common in temperate forests and are still the dominant management type in boreal forests (Kuusela, 1994; Puettmann et al., 2015; Kuuluvainen and Gauthier, 2018). Forest age structures are also influenced by other natural or anthropogenically caused disturbances such as fires, windthrows, droughts, pests and insect outbreaks (e.g. Soja et al., 2006; van Mantgem et al., 2009; Dore et al., 2010; Pan et al., 2011, 2013).

Changes in forest age structure in turn influence biophysical and biogeochemical interactions with the atmosphere, through changes in land surface properties such as albedo ~~, surface roughness, heat fluxes~~ and carbon uptake (e.g. Juang et al., 2007; Dore et al., 2010; Sun et al., 2010; Kirschbaum et al., 2011; Pan et al., 2011, 2013; Poorter et al., 2016; Erb et al., 2017). Forest age structure changes can influence the susceptibility to the environment and to environmental changes. It is, for example, hypothesised that the response of forests to increasing atmospheric CO_2 ceases as the forest matures, because other resources than CO_2, such as water and nutrients, become growth limiting (Körner, 2006).

It is crucially important to include forest age structures in estimates of the effects of land use on the global scale, primarily due to (1) the aforementioned large ~~extend~~ extent and substantial effects of forest undergoing changes in age structure; (2) the aim of global studies to include forest management effects in addition to anthropogenic land cover changes; and (3) because global studies usually only have a very coarse resolution. One example for such global studies ~~are the estimates~~ is the estimate of global land-use emissions for the annual global carbon ~~budgets~~ budget (Le Quéré et al., 2018), which ~~are~~ is conducted with dynamic global vegetation models (DGVMs). Here, 10 out of the 16 participating DGVMs account for wood harvesting. ~~Another example~~ Other examples are studies estimating ~~both biophysical and biogeochemical~~ biogeochemical and/or biophysical interactions between the land surface and the climate system. ~~These~~ Such studies are conducted with Earth system models (ESMs) including their land surface models (LSMs), many of which taking part in the coupled model intercomparison projects (CMIPs). Here, considerations of forest age structure might in particular be important for future scenarios that often include strong land-based mitigation measures, such as forest management and afforestation (e.g. in CMIP6's land use intercomparison project LUMIP, see Lawrence et al., 2016). Global studies, in particular the computationally expensive ESM simulations, inevitably need to be conducted on coarse horizontal resolutions, typically only about 0.5°to 2°. Land use will thus usually only happen on fractions of the grid-cells, creating the need to represent subgrid forest age structures. The importance of subgrid forest age structures is also underlined by recent studies stressing the role of forest (re-)growth for the historical and future terrestrial carbon uptake (e.g. Kondo et al., 2018; Krause et al., 2018; Yao et al., 2018) and by studies simulating smaller ~~land use~~ land-use emissions when accounting for secondary forests (e.g. Shevliakova et al., 2009; Yue et al., 2018a). Despite all this evidence, many DGVMs, and particularly also those used as LSMs in ESMs, do not account for subgrid forest age structures (Pongratz et al., 2017).

There are categorically different approaches of how subgrid forest age structures can be implemented in DGVMs, depending on whether these models are individual-/cohort-based or tile-based. In the class of individual- and cohort-based models (referred to as vegetation demographic models in Fisher et al., 2018), subgrid structures are inherently provided. Examples are ED-derivatives (Fisher et al., 2015, 2018), LPJ-Guess (Smith et al., 2001; Bayer et al., 2017), and the SEIB-DGVM (Sato et al.,

2007). In the (larger) class of tile-based models (also referred to as area-based in Smith et al., 2001), subgrid structures are not inherently provided. In these models each tile describes an average individual per plant functional type (PFT). Examples for this class of DGVMs are CABLE (Haverd et al., 2018), Class-CTEM (Melton and Arora, 2016), ISAM (Yang et al., 2010), JSBACH (Reick et al., 2013; Mauritsen et al., 2019), LM3 (Shevliakova et al., 2009), LPX-Bern (Stocker et al., 2014b), different versions of ORCHIDEE (Naudts et al., 2015; Yue et al., 2018b) and others. In our study we focus on the second class of DGVMs, as they are more commonly used as LSMs in ESMs. One reason that tile-based models are more commonly used is simply that they have lower computational costs. Another reason is their often historically conditioned top-down development, which facilitates a fully coupled execution within the corresponding ESM.

To ~~extent~~ expand tile-based DGVMs to represent subgrid forest age structures, two approaches have recently been developed. The ~~most~~ more frequently applied approach has been to increase the number of tiles in such a way that a certain number of age-classes or structurally similar stands can be distinguished. A pioneer study has been the paper by Shevliakova et al. (2009), using the model LM3 with a fixed number of in total 12 secondary land tiles for all PFTs and a similarity-based merging of tiles in order to maintain the number of tiles despite further land use/disturbances. Comparably, ORCHIDEE-MICT (Yue et al., 2018b) introduced a fixed number of six tiles per woody PFT, with tile merging upon exceeding pre-defined woody biomass boundaries. In ORCHIDEE-CAN three tiles per woody PFT with tile merging upon exceeding diameter thresholds have been used, while further within-stand structuring has been applied in each tile by accounting for a user-defined diameter distribution (Naudts et al., 2015). An increase of tiles has also been chosen in ISAM (Yang et al., 2010) and LPX-Bern (Stocker et al., 2014a, b); in these models, however, only one additional tile per PFT has been introduced in order to distinguish primary and secondary vegetation. A common drawback of the hitherto existing implementations is the missing traceability of the actual age of the forests as soon as tiles are merged. Merging of tiles, however, is a necessity when the number of age-classes is constrained by ~~computational~~ computation costs.

The alternative approach for extending the number of tiles to represent subgrid forest age structure in tile-based DGVMs is to keep the information about the forest structure in a separate module. For ORCHIDEE-FM (Bellassen et al., 2010), for example, ORCHIDEE has been coupled to a forest management module (FFM). FFM takes the tile wood increment calculated in ORCHIDEE as input, allocates the increment to tracked individual trees, conducts self-thinning and forest management, and feeds back the leaf area index (LAI), biomass and litter to the tile. A comparable coupling is described in Haverd et al. (2018), where the DGVM CABLE is coupled to the Population Orders Physiology (POP) module for woody demography and disturbance-mediated landscape heterogeneity (Haverd et al., 2014). POP has a detailed description of the forest structure and simulates the growth of age/size classes of trees competing for soil resources and light. For each forest tile, POP gets the stem NPP from CABLE and returns woody vegetation height, mortality and sapwood mass. Whilst such a use of a separate module principally enables tracking the exact age of the forest in a grid-cell, it has the drawback of using average tile information to compute ~~land–atmosphere interactions~~simulated processes, such as photosynthesis~~or soil moisture state. Feedbacks between stands of different ages and the environment~~ . Age-dependencies of these processes can thus not be represented.

In this paper we ~~try to~~ bridge the two approaches for extending tile-based DGVMs to represent subgrid forest age in the sense that we present a way to trace the actual age of the forests in a grid-cell despite following the first approach using a

restricted number of additional tiles and thus required merges. ~~This approach is therefore more accurate than the current way of implementing subgrid forest age structures by increasing the number of tiles and allows land–atmosphere interactions to be simulated in dependence of forest age.~~ The suggested approach is applicable for any tile-based DGVM, provided the tiles are structured in a hierarchical way. We describe the implementation of our approach in the DGVM JSBACH4 and use the new model version to conduct test simulations with different numbers of age-classes and age distribution schemes. Subsequently, we compare the different simulation results against observation-based data to ~~evaluate~~ investigate the compromise between computation costs and ~~accuracy~~error reduction.

2 Methods

2.1 JSBACH4

The DGVM JSBACH4 is used as LSM in the ICON-ESM (Giorgetta et al., 2018). ~~It~~ In addition, JSBACH4 is developed with a flexible interface, such that it is also usable within MPI-ESM1.2 (Mauritsen et al., 2019) and as a standalone model driven by climate data. JSBACH4 is a re-implementation of JSBACH3~~(Mauritsen et al., 2019)~~, the original LSM used in MPI-ESM1.2 (Mauritsen et al., 2019), but with a more flexible and extendable structure via a hierarchical representation of tiles (Fig. 1)~~, allowing different processes to be simulated on different levels of the hierarchy. Whilst JSBACH4 is a fully fledged DGVM, and most of the processes from JSBACH3 already have been ported to JSBACH4, some important processes still need to be implemented in~~. The implementations described in this paper are based on the current version (4.20p7), ~~in particular the representation of natural and~~ which includes most of the processes implemented in JSBACH3, such as land physics, photosynthesis, carbon allocation and natural disturbances, but is still lacking JSBACH3's representation of anthropogenic land cover change (Reick et al., 2013). ~~In order to better be able to represent forest re-growth, the JSBACH4~~ Furthermore, the current version does not provide an infrastructure for the horizontal exchange of properties among tiles, such as, for example, movement of area fractions from one PFT to another.

As an important amendment to the current version (4.20p7)~~used as basis in this paper has been amended by a dependency of the~~, we ported a new JSBACH3 development, which we implemented in a recent independent study (Naudts et al., in prep.): While previous JSBACH3 versions assumed a PFT-dependent but constant maximum leaf area index (LAI), that is the LAI value that can maximally be reached at the peak of a season, Naudts et al. (in prep.) introduced a dependency of the maximum LAI on the available leaf ~~carbon, which only recently has been implemented in JSBACH3 (Naudts et al., in prep.)~~biomass. Such a dependency is a prerequisite for simulating forest re-growth and thus for the introduction of age-classes.

2.2 ~~Subgrid age structure with tracing of forest age – general concept~~JSBACH4–FF

As outlined in the introduction, we ~~aim~~ aimed for a scheme that allows subgrid forest age structures to be introduced in hierarchical tile-based models in a computationally efficient way, ~~but~~ i.e. using a restricted set of age-classes, but nevertheless

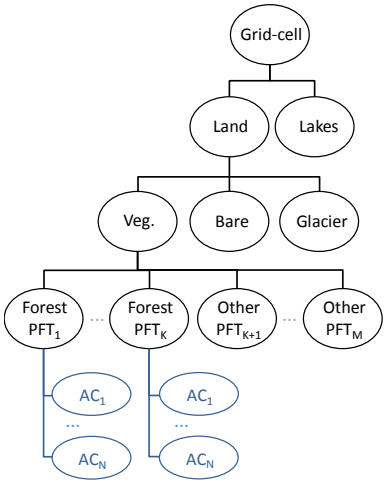

Figure 1. The hierarchical tile structure of JSBACH4. In our study, the default tile structure of JSBACH4 (in black) has been extended by a variable number N of forest age-classes (AC) below each of the K forest plant functional types (PFT; in blue).

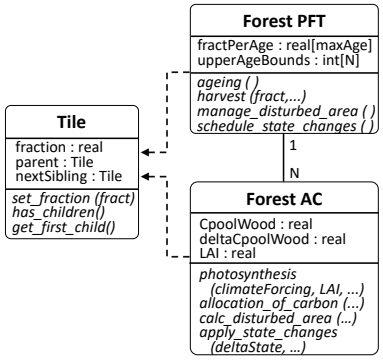

Figure 2. Unified Modelling Language ~~UML~~ diagram showing the relation between tiles, forest plant functional types (PFTs) and forest age-classes (ACs) in JSBACH4–FF, together with a selection of example state variables and functions (in italics). Forest PFTs and ACs are distinct types of tiles ~~in JSBACH4~~, with each PFT having N associated ACs. Each tile hosts certain state variables, for example the grid-cell fraction that it covers, as well as functions ~~in italics~~, for example to navigate the tile hierarchy. Different types of tiles add further ~~specific~~ variables and functions. Tiles representing ACs host variables and functions required for processes calculated on the lowest level of the tile hierarchy, such as photosynthesis or carbon allocation. Tiles representing PFTs host variables to maintain meta-information, for example ~~a vector (~~ the $fractPerAge$ ~~) containing~~ vector, that contains the fraction covered by ~~a certain~~ each age, i.e. one entry per year up to the maximum tracked age ($maxAge$). Furthermore, PFTs ~~they~~ host functions altering ~~concerning~~ more than one associated AC, for example ~~forest~~ ageing or harvest. ~~Depicted state variables and processes are exemplary.~~

with exact tracing of the age of the forest. ~~We thereby follow the mentioned approach of increasing the number of simulated tiles, but taking advantage of a hierarchical organisation of the tiles.~~

~~In tile-based models with a flat hierarchy the introduction of a subgrid age structure by increasing the number of tiles would require all processes previously executed on the PFT tile to also separately be simulated on each of the tiles representing age-classes. A hierarchical organisation of the tiles, such as provided in~~ For our new JSBACH4 ~~(Fig. 1), allows for a computationally more efficient way of introducing age-classes, because it makes it possible to choose on which level of the hierarchy processes are simulated. With a hierarchical organisation,~~ git feature "forests" (JSBACH4–FF) we took advantage of the existing hierarchical tile organisation of JSBACH4, which allows to introduce different processes and associated state variables ~~can be located~~ on different levels of the tile hierarchy (Fig. 2). ~~Thus, it is not a prerequisite any more that all processes previously executed on the PFT tile are simulated on each age-class tile. Now, only those processes~~ Already existing processes which are specific to the development of an age-class, such as photosynthesis and carbon allocation, ~~need to be executed on that~~ are still executed on the leaves, i.e. now per age-class. ~~All~~ However, processes related to several age-classes, such as ~~harvesting, ageing or required merges, are located~~ natural disturbances and the newly introduced ageing and harvesting processes, are implemented on the PFT level, which ~~manages~~ we use to manage associated age-classes ~~. Due to the hierarchy, moreover,~~ and to maintain meta-information ~~can be maintained on the PFT level. This latter aspect enables to trace the exact age of the forest up to a certain maximum age $maxAge$ despite only simulating a much smaller number N of age-classes (Fig. 2)~~about the forest age structure.

~~JSBACH4's new git feature "forests" (~~In JSBACH4–FF ~~) introduces an implementation of subgrid age structure following Section ??. For this purpose~~ we introduced a fixed user-defined number N of age-classes ~~is~~ pre-set in the configuration file for all forest PFTs (Fig. 1). In addition, ~~the upper-bound of each~~ a to be pre-defined upper age bound per age-class AC_M ~~($maxA_M$~~ ($maxA_K$) as well as ~~the~~ a total maximum age ($maxAge$) ~~need to be pre-defined~~were introduced. $maxAge$ determines the oldest age up to which the age ~~per~~ of an area is tracked, i.e. the length of the $fractPerAge$ vector ~~in each forest PFT~~ (Fig. 2). Area fractions with ages exceeding $maxAge$ are not further distinguished and are refereed to as old-grown forest. For a maximum age of 150 years, for example, each forest PFT would contain a vector with length 150 to track the exact age of the entire forest area up to 150 year old forest. Each AC_K covers a certain interval of years [~~$maxA_{M-1}$, $maxA_M$~~$maxA_{K-1}$, $maxA_K$) (Fig. 3), with the youngest AC (AC_1) always covering the range of year 0 to 1, and the oldest AC_N covering all forest older than $maxA_{N-1}$, i.e. [$maxA_{N-1}$, INF), with $maxA_{N-1} \leq maxAge$.

In JSBACH4–FF ~~different processes are implemented that~~ we implemented three processes on the PFT level which can cause shifts of area fractions from one AC to another (Fig. 3), each tracking changes in age fractions in the $fractPerAge$ vector.

Ageing The ~~ageing of forests happens annuallyand affects the oldest year in each AC~~newly implemented process of forest "ageing" happens annually: upon ageing each tracked forest fraction gets one year older. Yet, a shift from one age-class to the next age-class only happens for the area of the oldest age ($maxA_{K-1}$-1) of an age-class AC_{K-1}, i.e. only the forest area which upon getting one year older ~~the fraction of forests having age $maxA_{M-1}$~~exceeds the upper age bound $maxA_{K-1}$ of the AC_{K-1} needs to be shifted into AC_K. Thanks to the tracking of the age in the $fractPerAge$ vector, the exact area fraction with age $maxA_{K-1}$-1 ~~will shift from AC_{M-1} into AC_M~~ is known.

Harvest In the current version, ~~harvest is implemented~~ we implemented harvest as a clear-cut of a ~~fraction of the oldest available ACand~~ certain fraction of an AC, which can happen annually. Harvest causes a shift of the harvested fraction of the affected AC to the youngest AC. Since the exact age of each forest fraction is tracked in the $fractPerAge$ vector, age-based harvest rules can be specified.

Disturbances ~~The implemented disturbances (~~Following JSBACH3 (Brovkin et al., 2009) wind and fire ~~)~~ disturbances can happen daily in JSBACH4 and are assumed to clear certain area fractions of vegetation~~, as assumed in JSBACH3 (Brovkin et al., 2009)~~. In JSBACH4–FF disturbances ~~cause~~ were partly re-implemented. While the calculation of the disturbed area is still conducted on each leaf, i.e. on each AC ($calc\_disturbed\_area$ in Fig. 2), the movement of area between ACs is managed on the PFT level ($manage\_disturbed\_area$ in Fig. 2). This separation was required since the state variables used to determine the disturbed area, such as available fuel, need to be derived on the lowest layer of the hierarchy. Disturbances are realised as shifts of fractions of affected ACs to the youngest AC (AC_1).

~~These three processes are managed on the PFT level, where the exact forest age fractions are tracked. Each initiated shift entails a redistribution of forest carbon and a re-determination of other affected state variables of the involved ACs, which are directed and scheduled~~

Since JSBACH4 so far does not provide the infrastructure for the horizontal exchange of properties among tiles (Section 2.1), we had to implement such an infrastructure in JSBACH–FF, redistributing area fractions and associated state variables such as the carbon pools or the maximum LAI. This redistribution has been realised in two steps: in the first step, each of the three processes described above determines required redistributions on the PFT level ~~but exerted on the ACs. When a certain area (fa) is~~ ($schedule\_state\_changes$ in Fig. 2) according to Eq. 1 and Eq. 2. Here, fa is the area fraction moved from one AC to another, e.g. upon ageing~~, each affected state variable V_T of the target AC_T needs to be updated. V_T' is obtained by weighting the values V_S of the~~ ; V_S is the value of the state variable of the source AC_S and $delta\_V_S$ and $delta\_V_T$ are the scheduled changes of the state variable on the source AC_S and ~~V_T of~~ the target AC_T~~with respect to the ratio of incoming (fa) to current area (~~, respectively.

$$delta\_V_S = delta\_V_S - (V_S \cdot fa) \tag{1}$$

$$delta\_V_T = delta\_V_T + (V_S \cdot fa) \tag{2}$$

In the second step, the redistributions are applied on the ACs ($apply\_state\_changes$ in Fig. 2) according to Eq. 3. Here, V_{AC} represents the affected state variable of the age-class AC, $delta\_V_{AC}$ the scheduled change, fa is the incoming and fc ~~):~~ the current area of the age-class AC.

$$V_{TAC}{}' = \frac{V_T \cdot fc + V_S \cdot fa}{(fc + fa)} \frac{V_{AC} \cdot fc + delta\_V_{AC}}{(fc + fa)} \tag{3}$$

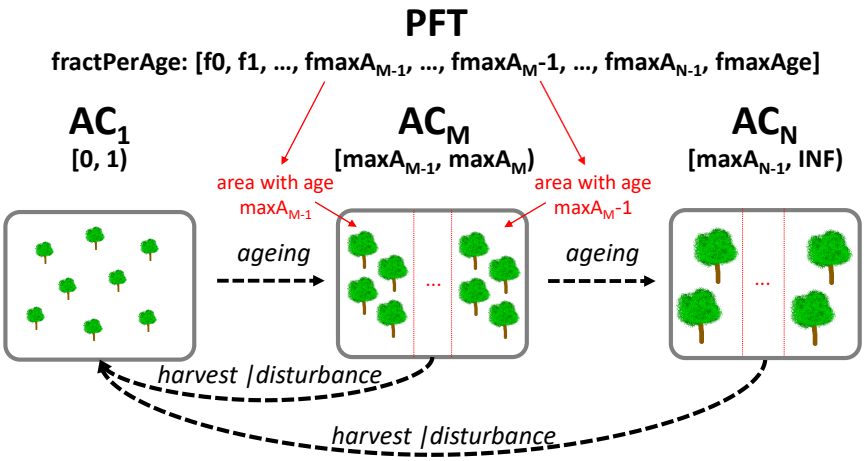

Figure 3. Visualisation of forest age-class (AC) boundaries, the $fractPerAge$ vector, and processes causing shifts from one AC to another in JSBACH–FF. Each AC covers a certain interval of ages. The first AC contains all forest younger than one year; an arbitrary AC~~$_M$~~$_K$ covers [~~$maxA_{M-1}$~~$maxA_{K-1}$,~~$maxA_M$~~$maxA_K$), i.e. the ages in the right-open interval of the upper age boundary of the previous AC (~~$maxA_{M-1}$~~$maxA_{K-1}$) and its own upper age boundary (~~$maxA_M$~~$maxA_K$); finally the last class AC$_N$ covers all forest older than and including the upper age boundary of the next younger class ($maxA_{N-1}$), with $maxA_{N-1}$ being smaller or equal to the total maximum age ($maxAge$). The information on the area covered by the different ages (indicated in red) is ~~only known to~~ tracked in the $fractPerAge$ vector of the associated forest PFT~~($fractPerAge$ in Fig. 2)~~. Three processes can lead to movement of area fractions among ACs: ageing leads to movement of the fraction exceeding the maximum age of an AC; harvest and disturbances lead to movement of fractions to the first AC.

2.2 Simulation set-up and measures of model performance

The main purpose of JSBACH are global applications, often in a mode coupled to an ESM. Therefore, we assess the ability of different set-ups without and with different numbers of age-classes to reproduce the annual cycle and large-scale spatial patterns of gross primary production (GPP), forest LAI and forest above-ground biomass (AGB) by comparing simulated variables against global observation-based products for different seasons and regions. We conducted simulations following a protocol described below (Section 2.2.2), with the aim to simulate actual 2010 forest age distributions and forest states. Forest ~~gross primary production (GPP)~~GPP, forest LAI and forest ~~above-ground biomass (AGB)~~ AGB simulated for 2001 to 2010 were compared against GPP, LAI and AGB data based on observations using a normalised root mean squared error (NRMSE; Section 2.2.5). In addition, we created Taylor diagrams for each variable, season and region (see Figures S5.5–S5.11 in the supplementary).

2.2.1 Observation-based data

We used ~~GPP and LAI data for the year~~ 2010 ~~as derived in Tramontana et al. (2016). This data already had~~ MODIS LAI (Myneni et al., 2002) and GPP data obtained from machine learning methods trained on flux-tower measurements (Tramontana et al., 2016). These LAI and GPP datasets had already been mapped to JSBACH's forests PFTs in a previous study (see supplementary of

Nyawira et al., 2016). From ~~this data~~ these datasets seasonal means were calculated and expressed per forest area by dividing them by the sum of the forest cover fractions used for the JSBACH4–FF simulations (Section 2.2.2). The AGB per forest area (Avitabile et al., 2016) was downloaded from the GEOCARBON data portal (www.bgc-jena.mpg.de/geodb/projects/Data.phd) and remapped to T63 using the conservative remapping operator of the climate data operators (CDOs, version 1.9.5). Figures S4.2–S4.4 in the supplementary show maps of the pre-processed observation-based data.

2.2.2 General simulation set-up

We conducted simulations with JSBACH4 (4.20p7) feature/forest in standalone mode hosted within the MPI-ESM environment (see supplementary material S1 for further information). We used JSBACH's default set-up comprising 12 PFTs, of which 4 are of a forest type: Tropical evergreen and deciduous forest (TE and TD) and extratropical evergreen and deciduous forest (ETE and ETD). Simulations started in 1860 from scratch, i.e. with empty vegetation carbon stocks, and were run up to 2010. Empty carbon stocks are a simplification used in the absence of global knowledge on the state of the forest in 1860, but have no influence on our results, since in simulations with JSBACH4 (4.20p7) LAI, GPP and AGB only depend on the age since the last clearing event, not on the history before that. The starting date of 1860 was chosen such that it covers at least one full cycle of regrowth, as the oldest age resolved in the simulations matches that of the observation-based data (Poulter et al., 2018). We used T63 resolution (192 longitudes x 96 latitudes; 1.9° × 1.9°), a climate forcing based on GSWP3 (Kim et al., 2012) and CO_2 from the collection of greenhouse gas concentrations for CMIP6 (Meinshausen et al., 2017). To obtain forest age distributions comparable to those observed for 2010 (Poulter et al., 2018), harvest was conducted following prescribed maps (Section 2.2.4) and natural disturbances were switched off in order to not additionally alter forest age. The simulations were conducted with a static land-use map for 2010, based on TRENDYv4 JSBACH3 output (Le Quéré et al., 2015). The TRENDYv4 JSBACH3 simulation started from a potential vegetation map extrapolated from remote sensing (Pongratz et al., 2008) and was forced by the Land-use Harmonization dataset LUH1 (Hurtt et al., 2011). We conducted simulations with different numbers and distributions of age-classes (Section 2.2.3). All simulations were conducted on Mistral, the High Performance Computing system of the German Climate Computing Center (DKRZ), using an identical number of CPUs.

2.2.3 Simulated number of age-classes and age distribution schemes

Table 1 lists the conducted simulations. We used different numbers of age-classes and two different age distribution schemes described below. The selected numbers of age-classes are ~~exemplary only~~arbitrary; however, the finest resolution into 15+1 age-classes was motivated by the ~~discretisation of the age map (Section 2.2.4)~~age map discretisation in Poulter et al. (2018) using 15 age-classes that cover 10 years each. In addition to simulations with age-classes, we performed one simulation only using PFTs, i.e. without age-classes. ~~In this simulation we used the same harvest fractions prescribed as in the simulations with age information, but harvest was applied as done in JSBACH3 (Reick et al., 2013), i.e. by simply diluting the wood carbon of the harvested PFT tiles.~~

The two applied age distribution schemes are defined as follows:

EAS The equal age-spacing (EAS) distribution scheme spreads the age-classes evenly over the age space. For example, a maximum traced age of 150 years distributed evenly over 10+1 age-classes (EAS11 in Table 1) results in age-classes covering 15 years with the following upper age bounds: 1, 16, 31, 46, ..., 136, INF. This distribution was motivated by the equal spacing applied in the forest age map by Poulter et al. (2018).

IAS The increasing age-spacing (IAS) distribution scheme uses an increasing age range covered with increasing age, i.e. younger age-classes cover smaller intervals in the age space than older age-classes. The upper age bound of a forest age-class ~~M~~ ~~(uLim$_M$~~K (uLim$_K$) is defined following Eq. 5.

$$\text{spacing} = \frac{maxAge}{\sum_{i}^{N-1} i} \frac{maxAge}{\sum_{i=1}^{N-1} i} \tag{4}$$

$$\text{uLim}_{MK} = \begin{cases} 1, & \text{if K=1} \\ \text{INF}, & \text{K = N} \\ \text{uLim}_{K-1} + \text{int}(\text{spacing} \cdot K), & \text{else} \end{cases} \tag{5}$$

With $maxAge$ being the maximum age and N being the number of age-classes. A maximum age of 150 years distributed with IAS over 10+1 age-classes (IAS11 in Table 1) results in age-classes with the following upper age bounds: 1, 3, 8, 16, 26, 39, 55, 74, 95, 119, INF. This second distribution scheme was motivated by the fact that young forests usually have larger incremental changes in most variables than old ones (see e.g. Amiro et al., 2006; Martínez-Vilalta et al., 2007; Leslie et al., 2018).

Both distribution schemes are applied in a static way, i.e. the age-class boundaries do not change during runtime. Figure 4 shows the division into age-classes resulting for the different simulation set-ups for an example grid-cell in Canada.

Table 1. Conducted simulations with number of age-classes and applied age distribution scheme. The "+1" in the number of age-classes refers to the youngest age-class, which always covers the years 0 to 1 in JSBACH4–FF.

Simulation name	PFT	EAS03	IAS03	EAS06	IAS06	EAS08	IAS08	EAS11	IAS11	EAS13	IAS13	EAS16	IAS16
Number of age-classes	–	2 + 1	2 + 1	5 + 1	5 + 1	7 + 1	7 + 1	10 + 1	10 + 1	12 + 1	12 + 1	15 + 1	15 + 1
Age distribution scheme	–	EAS[a]	IAS[b]	EAS	IAS	EAS	IAS	EAS	IAS	EAS	IAS	EAS	IAS

[a] EAS: equal age-spacing; [b] IAS: increasing age-spacing

2.2.4 Harvest maps

Harvest maps were derived such that the observed 2010 forest age distribution given by Poulter et al. (2018) is reached in the final simulation year ~~2010.~~ 2010 for simulations using age-classes. The observed forest age map of course not only reflects forest harvest, but all processes influencing the age of a forest, i.e. also natural disturbances and anthropogenic land cover change. Because assigning the observed age structure to forest harvesting vs natural disturbances vs anthropogenic land cover

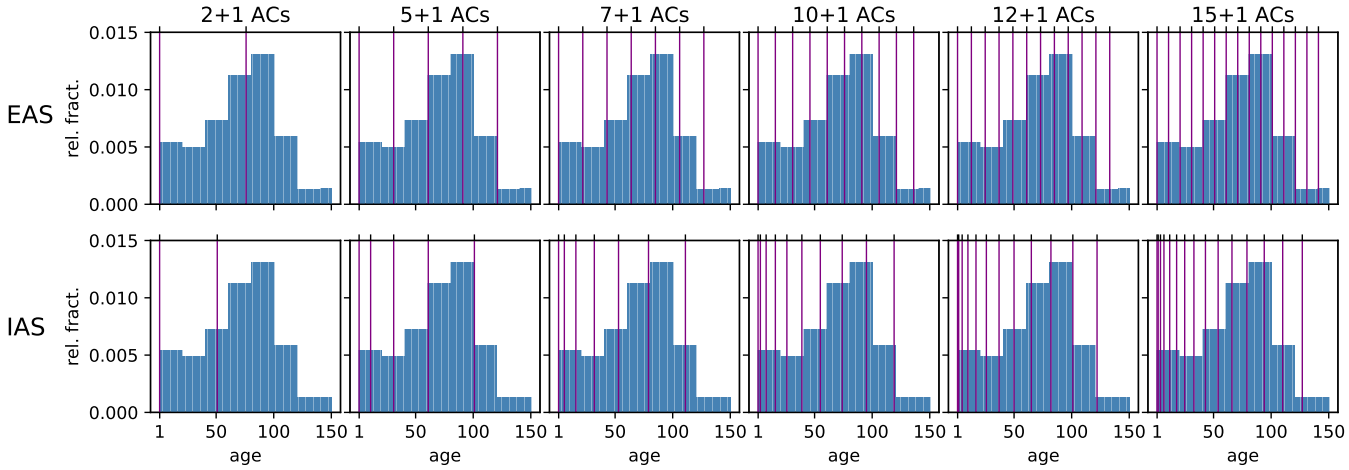

Figure 4. Division into age-classes (ACs) for the different simulations listed in Table 1 (EAS: equal age-spacing; IAS: increasing age-spacing). Purple lines mark the upper age boundary of each age-class. The blue bars show the relative fraction for each year resulting for an example cell in Canada (lon = 286.875, lat = 47.5639) in the simulation year 2010. Note that no harvest was conducted in the final simulation year 2010, therefore the smallest age-class is empty.

change would come with uncertainties and is not relevant for our study (as only the affected fraction of an age-class matters, independent of the underlying causes), we apply only forest harvest to obtain the observed age distribution.

The map by Poulter et al. (2018) provides a grid with 0.5°resolution of the global forest age distribution of ~~4 forest PFTs(needleleaf evergreen and deciduous~~four forest PFTs: needleleaf evergreen (NE) and needleleaf deciduous (DE), as well as broadleaf evergreen ~~and deciduous) on a grid with 0.5resolution~~(BE) and broadleaf deciduous (BD). The map uses a discretisation into 15 age-classes, covering 10 years each, with the last class containing all area with an age >140 years. In a pre-processing step, the map was remapped to T63 using the conservative remapping operator of the CDOs. Subsequently, the ~~PFTs from the map were scaled to~~ area sums of the two evergreen and the area sums of the two deciduous PFTs from Poulter et al. (2018) were used to derive the age-class maps for JSBACH's ~~PFT cover fractions. From these scaled~~ evergreen and deciduous PFTs, respectively, following Eq. 6:

$$\text{cf\_age}_i\text{\_PFT}_k = (\text{cf\_age}_i\text{\_}N + \text{cf\_age}_i\text{\_}B) \cdot \frac{\text{cf\_PFT}_k}{\sum_{i=1}^{15}(\text{cf\_age}_i\text{\_}N + \text{cf\_age}_i\text{\_}B)} \tag{6}$$

where i is one of the 15 age-classes from Poulter et al. (2018) and k refers to one of the four forest PFTs of JSBACH. N (needleleaf) and B (broadleaf) refer to the PFTs in Poulter et al. (2018), where either both are evergreen (in case that PFT_k is evergreen) or both are deciduous PFTs (in case that PFT_k is deciduous).

From these age maps, we derived harvest maps for each simulation year such that the simulated age distribution in simulations with age-classes conforms with the observed one in 2010, assuming that the fractions given by Poulter et al. (2018) are equally

distributed over the ten years covered by each age-class (see supplementary material S2 for more details). In ~~each simulation year the to be harvested fraction was read from the harvest map for that simulation year and the according fraction was transferred from the oldest to the youngest forest age. In~~ the first (1860) and in the last simulation year (2010) no harvest was conducted.

In different simulation types – with or without age-classes – the same harvest maps were used, but different forest management schemes were applied. In simulations with age-classes, a clear-cut according to the fractions in the harvest map was taken from the oldest age-class. In the simulation without age-classes, the PFT simulation, we used the same harvest fractions as in the simulations with age-classes, but harvest was applied as done in JSBACH3 (Reick et al., 2013), i.e. by diluting the wood carbon of the harvested PFT tile.

2.2.5 NRMSE

We calculated the area-weighted root mean squared error (RMSE) according to Eq. 7 based on difference maps between 'OBS', the observation-based data (Section 2.2.1), and 'SIM', the results of each simulation (see Table 1). The RMSE was calculated for 2001-2010 simulation output averages, separately for each variable 'V' and three selected regions 'R'. Each selected region defines a latitudinal band, including all forested land on a subset of the 96 latitudes and the entire 192 longitudes (see Table 2 for the regions, their latitudinal boundaries and the latitude indices b1 and b2). For GPP and LAI the four seasons 'S' (DJF, MAM, JJA, SON) were calculated separately. The RMSE for each variable, region and season was subsequently normalised with the range (Max-Min) observed for that variable, region and season (Eq. 8).

Table 2. Selected regions used for the comparison of simulation results and observation-based data and their latitudinal boundaries and indices.

Abbr.	Region	max lat	b1	min lat	b2
BOR	Boreal	90°	1	50°	21
NH-TMP	Northern Hemisphere Temperate	50°	22	30°	32
TROP	Tropical	30°	33	-30°	64

$$\mathrm{RMSE}_{\mathrm{V,S,R}} = \sqrt{\frac{\sum_{\mathrm{k=1}}^{192}\sum_{\mathrm{m=b1}}^{\mathrm{b2}}\left((\mathrm{OBS}_{\mathrm{V,S,lon(k),lat(m)}} - \mathrm{SIM}_{\mathrm{V,S,lon(k),lat(m)}})^2 \cdot \frac{\mathrm{AREA}_{\mathrm{lon(k),lat(m)}}}{\mathrm{AREA}_{\mathrm{R}}}\right)}{192 \cdot (\mathrm{b2\text{-}b1+1})}} \tag{7}$$

$$\mathrm{NRMSE}_{\mathrm{Max\text{-}Min,V,S,R}} = \frac{\mathrm{RMSE}_{\mathrm{V,S,R}}}{\mathrm{Max}(\mathrm{OBS}_{\mathrm{V,S,R}}) - \mathrm{Min}(\mathrm{OBS}_{\mathrm{V,S,R}})} \tag{8}$$

To more easily assess changes in performance when increasing the number of age-classes the different $\mathrm{NRMSE}_{\mathrm{Max\text{-}Min}}$ values were subsequently aggregated per variable by averaging over the regions (for AGB) and in addition over the seasons (for GPP and LAI), using equal weights.

2.2.6 Computational costs

In addition to determining the NRMSE for different variables, we also determined the computation costs of the different set-ups. We calculated the average CPU time recorded for the simulation years 2001-2010. Whilst absolute computation times are of less interest here, particularly since JSBACH4 is still highly under development and currently does not reach the targeted performance, relative differences among the set-ups depict the costs of the introduction of subgrid forest age structures.

3 Results and Discussions

Having forest age-classes in JSBACH4–FF facilitates a finer discretisation in each grid-cell and ~~enables the~~ is a precondition for any implementation of age-based forest management. The number of age-classes in JSBACH4–FF is flexible, and in the following we describe the evaluation of simulation results using different numbers of age-classes and age distribution schemes and discuss the compromise between computation costs and ~~accuracy~~error reduction, when selecting a certain number of age-classes (Section 3.1). Subsequently, we more closely examine differences between ~~a simulation with an exemplary~~ an example simulation with a selected number of age-classes and a simulation only using PFTs, i.e. without age-classes, to investigate the benefits of having age-classes in JSBACH4–FF (Section 3.2). Finally, we discuss assets and drawbacks of alternative schemes introducing age-classes in tile-based DGVMs (Section 3.3).

3.1 Evaluation

In this section we use the $NRMSE_{Max\text{-}Min}$ for different regions/seasons as aggregated measure to compare the different simulation set-ups. A closer examination between a simulation with and without age-classes including a spatially explicit comparison follows in Section 3.2.

Introducing age-classes improves the comparison to observation-based data for nearly all compared variables, regions and seasons (Fig. 5), with the only notable exception of the AGB in the boreal region, where the PFT simulation was more similar to the observation-based data than the simulations with age-classes (Fig. 5c). For most comparisons, the $NRMSE_{Max\text{-}Min}$ indicates a small but distinct improvement over not representing a forest age structure for all simulated numbers of age-classes and both age distribution schemes.

Averaging the $NRMSE_{Max\text{-}Min}$, giving each region and each season the same weight, results in an $NRMSE_{Max\text{-}Min}$ ~~exponentially~~ decreasing with the number of age-classes for GPP and LAI (Fig. 6a and b) but saturating for larger numbers of age-classes. This shape holds for all regions, with a faster decrease and an earlier saturation for the northern hemisphere temperate and tropical regions than for the boreal region (Fig. S3.1a-f). The $NRMSE_{Max\text{-}Min}$ for AGB shows a slowly saturating increase with the number of age-classes for the boreal region (Fig. S3.1g) and only small differences among the different numbers of age-classes in the northern hemisphere temperate and the tropical regions (Fig. S3.1h and i). The observed increase in $NRMSE_{Max\text{-}Min}$ for the boreal AGB is due to an increased underestimation when accounting for more young forest, as is also discussed below (Section 3.2). Apart from the boreal AGB comparison, all comparisons show a smaller $NRMSE_{Max\text{-}Min}$ for simulations using

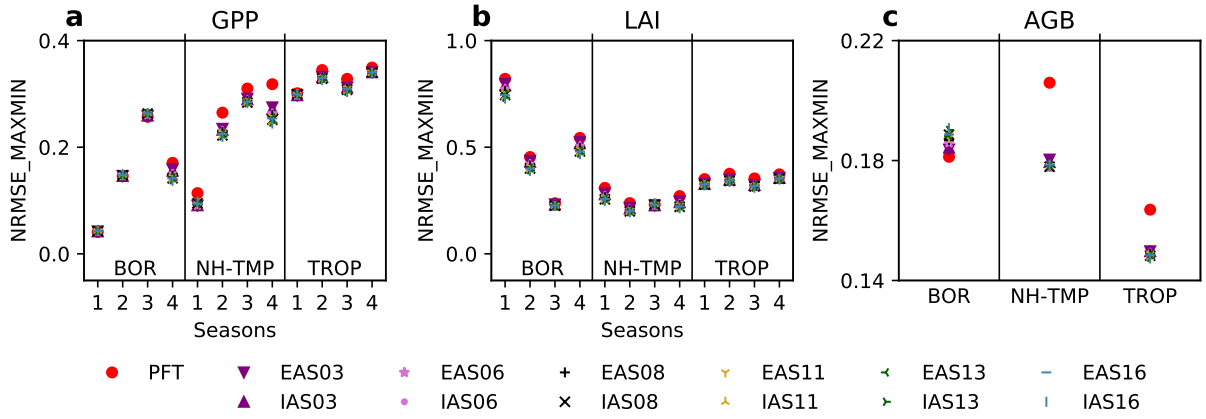

Figure 5. Evaluation of the conducted simulations (Table 1) with observation-based data by means of the normalised root mean squared error (NRMSE$_{\text{Max-Min}}$(, Section 2.2.5). Depicted are calculated NRMSE$_{\text{Max-Min}}$ (Section 2.2.5) values for each simulation for the gross primary production (GPP; panel **a**), the leaf area index (LAI; panel **b**) and the above-ground biomass (AGB; panel **c**). The NRMSE$_{\text{Max-Min}}$ is calculated as the root mean squared error of observation-based data and simulation results, normalised with the range (Max-Min) of the according variable for each of the selected regions (Table 2); and for LAI and GPP also for each of the four seasons.

the IAS distribution scheme (Fig. 6 and Fig. S3.1), i.e. a distribution applying an increasing age space (visualised in Fig. 4). This ~~increase in performance~~ decrease in NRMSE$_{\text{Max-Min}}$ is due to the finer discretisation of younger age-classes ~~with~~ which have fast-changing LAI and GPP, which ~~saturate~~ saturates for older age-classes (see e.g. Fig. 7 for ~~GPP~~LAI). In summary, a finer discretisation, particularly of the younger age-classes, is leading to values closer to the observation-based data, albeit the benefit of increasing the number of age-classes is slowly saturating towards larger numbers of age-classes (Fig. 6).

We performed the averaging of the NRMSE$_{\text{Max-Min}}$ to more easily assess ~~the differences in performance among the different numbers of age-classes and the two age distribution schemes~~differences among the simulations performed (Table 1). For this, we equally weighted the selected regions, because we wanted to equally account for these regions, which strongly differ in simulated PFTs and land–atmosphere interactions. Alternatively, we could have weighted the regions by area, which would have lead to an increasing weight of the tropical region, and thus to an earlier saturation of the NRMSE$_{\text{Max-Min}}$ with increasing age-classes.

Comparisons of required CPU times show a ~~linear~~ near-linear increase with an increased number of age-classes (Fig. 6d) and neither a difference between the two age distribution schemes, nor ~~an~~ a striking offset as compared to the PFT simulation. ~~This behaviour~~ A near-linear increase with an increasing number of age-classes was expected, since the processes requiring most of the computing time, such as the calculation of photosynthesis, carbon allocation and respiration, are conducted on the age-classes. The absence of ~~an~~ a striking offset comparing the PFT simulation with the age-class simulations indicates that the introduced organisational overhead on the PFT level in simulations with age-classes~~is not substantial~~, i.e. tracing of the exact forest age and redistributions of area fractions and other state variables among tiles, is not dominating the computation times.

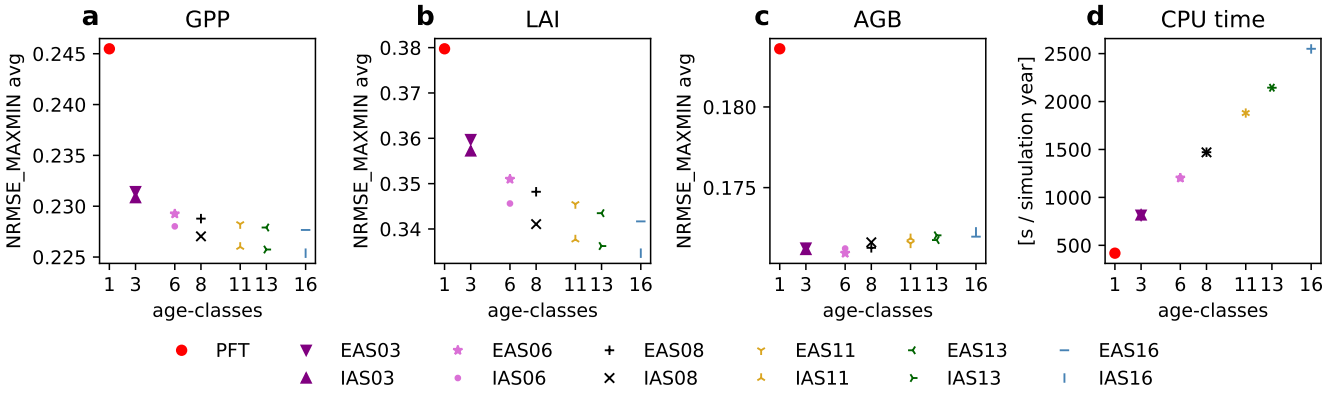

Figure 6. Change in the normalised root mean squared error ($NRMSE_{Max\text{-}Min}$, Section 2.2.5) and in the CPU time when increasing the number of age-classes. Panel **a** to **c** show the averaged $NRMSE_{Max\text{-}Min}$ (see also Fig. 5). Averaging has been conducted giving equal weights to all selected regions (Section 2.2.5) for AGB (panel **c**) and in addition to all four seasons for GPP and LAI (panel **a** and **b**). Figure S3.1 in the supplementary material shows the same data separately for each region. Panel **d** shows the computation time required per simulation year averaged over the years 2001-2010.

As expected, the optimal number of age-classes is a compromise between computation costs and ~~accuracy~~reduction of the error, which is a logical and commonly observed aspect when dealing with discretisation in models (see e.g. Nabel, 2015; Fisher et al., 2018). In the end, the choice of the number of age-classes to be used in a JSBACH4–FF simulation will depend on the application. Simulations comparing different forest management regimes in detail might, for example, aim for a fine discretisation, while more general simulations covering long time-spans might tend to aim for fewer age-classes. For the remaining parts of this manuscript, one set-up has been selected as an illustrative example: IAS11 (see Table 1), i.e. the simulation with 10+1 age-classes and the age distribution scheme with increasing age space. This set-up is a compromise between ~~accuracy of~~ the error reduction for GPP and LAI ~~representation~~ comparisons on one hand and ~~boreal AGB representation and~~ CPU time on the other. However, the main findings will not depend on the exact number of age-classes selected, particularly not as long as they are in the saturation part of the ~~exponential~~ decreasing function regarding GPP and LAI comparisons.

3.2 On the benefit of having age-classes

The evaluation with observation-based GPP, LAI and AGB data showed that simulations with age-classes were closer to the observation-based data for nearly all comparisons (Fig. 5 and Fig. 6). Spatially explicit comparisons of the results from the PFT simulation and observation-based data ("OBS-PFT" in Figs. S4.2–S4.4, column 2) indicate several areas of underestimation (red) and of overestimation (blue) for all variables. In Fig. 7 we compare results of a JSBACH4–FF simulation with age-classes, a simulation only using PFTs, as representative for a DGVM without forest age structures, and the observation-based data of ~~summer (JJA) GPP~~spring (MAM) LAI. The comparison is done for illustrative grid-points that were selected to cover areas of both over- and underestimation and to represent different typical land-use histories or forest management regimes,

resulting in different age distributions: a grid-point with an age distribution matching historically continuous clear-cuts and some more recent changes in land-use intensity in Germany (Fig. 7a); a grid-point with uniform age distribution resulting from a continuous, steady clear-cutting in Finland (Fig. 7b); a grid-point with untouched old-grown forest on one hand and young managed forest on the other hand in India (Fig. 7c); a grid-point with intensive harvest/disturbances in the south-east of the US (Fig. 7d); a heavily deforested example in east South America resulting nearly exclusively in young forest (Fig. 7~~e~~f); a grid-cell with recent afforestation in China (Fig. 7~~f~~e) and a grid-cell with pre-dominantly old-grown forests in central Africa (Fig. 7g). In general, the simulation with age-classes results in smaller GPP, LAI and AGB values (Fig. 7 and Figs. S4.2–S4.4, column 3), which is expected, since GPP, LAI and AGB are non-linearly increasing and saturating with age (see e.g. Fig. 7). Therefore, a harvested age-less forest in the PFT simulation has higher values for these variables than a fraction weighted average of an age-structured forest in the same grid-cell in the simulation with age-classes (Fig. 7). Since the simulation with age-classes generally results in smaller GPP, LAI and AGB values, overestimations can get alleviated, causing a decrease in the $NRMSE_{Max\text{-}Min}$, while underestimations can get more severe, causing an increase in the $NRMSE_{Max\text{-}Min}$. The comparison of the differences between observation-based data (OBS) and the PFT simulation results on one hand, and OBS and the IAS11 simulation results on the other hand, accordingly shows higher similarity in several areas where the PFT simulation indicated overestimation (areas which are blue in column 2 and 4 in Figs. S4.2–S4.4) and less similarity in some areas with underestimation (areas which are red in column 2 and 4 in Figs. S4.2–S4.4). Fig. 7 shows several grid-point examples with increased underestimations of ~~summer GPP~~ spring LAI (Fig. 7 panel ~~b and c~~a and e), reduced overestimations (panel ~~a and d~~b and c) and grid-points where the previous overestimation is now replaced by a slight ~~(Fig. 7e) or an equally large~~ underestimation (Fig. 7 panel d and f). Globally, reduced overestimations get particularly visible for LAI in the east of South America, and for several seasons also for example over China, North America and Europe (Fig. S4.3d,h,i,p). For GPP (Fig. S4.2d,h,i,p) and AGB (Fig. S4.d) the pattern is more mixed, with reduced overestimations particularly in the east of North America and China and partly for the east of South America. In addition, there are several areas of under- and overestimation which are very similar in the two simulations (areas coloured in column 2 and white in column 4 in Figs. S4.2–S4.4). These are particularly areas with pre-dominantly old-grown forests, i.e. without a distinct age-structure, such as central Africa, central Amazon and Siberia, where the PFT and the age-class simulation led to similar results (see e.g. Fig. 7g). In summary, simulations using age-classes led to a decrease in the simulated GPP, LAI and AGB values due to their non-linear increase with a saturation for older ages. This caused a decrease in the $NRMSE_{Max\text{-}Min}$ in areas where the PFT simulation was biased high and an increase in the $NRMSE_{Max\text{-}Min}$ in areas where the PFT simulation was biased low. Thus, if such a forest age-structure would be implemented in a DGVM being predominately biased low, the difference to the observation-based data could increase. In this context, also caveats regarding the observation-based data themselves need to be raised. A known caveat regarding MODIS LAI data is the problem of reflectance saturation in dense canopies making the reflectance insensitive to changes in LAI (Myneni et al., 2002). This problem which is particularly relevant to the tropical region could lead to a general high bias of the model compared to the observation-based data. However, since this problem is more typical for denser, old-grown forests, this high bias would also occur in simulations with age-classes. Regarding the GPP data from Tramontana et al. (2016), a recent study by Besnard et al. (2018) criticised that the applied empirical upscaling techniques do not directly consider forest age, making it unclear how well they can capture

age-related dynamics. In their study, Besnard et al. (2018) advocate the development of alternative global datasets considering forest age as a predictor.

~~Importantly, besides the slight increase in accuracy, the main gain of JSBACH4–FF is the additional functionality by~~ Importantly, besides the error reduction observed for JSBACH4–FF simulations, the newly implemented forest age-structure ~~.~~ ~~The age-structure~~ adds further functionality to JSBACH4–FF. It facilitates keeping the coarse resolution required in ESM simulations while nevertheless capturing some of the sub-grid scale heterogeneity that is important to better resolve several of the simulated processes. ~~Particularly~~Furthermore, the forest age-structure ~~enables the implementation of different~~ is a precondition for any implementation of forest management regimes while simultaneously accounting for differences in the productivity and the standing stocks. The grid-point examples shown in Fig. 7 highlight the relevance of a distinction of age-classes, since they demonstrate the non-linear relationship between ~~GPP~~ LAI and forest age. A similar relationship can be found for AGB and ~~LAI~~GPP. Consequently, the ability to distinguish age-classes enables a more accurate simulation of the biogeochemical consequences of land use and particularly prescribed harvest regimes. For example, harvesting of younger age-classes will lead to lower land-use emissions, as also described in other studies (e.g. Shevliakova et al., 2009; Yue et al., 2018a). Similarly, being able to distinguish forest age-classes will also affect biophysical land–atmosphere interactions, since younger forests, for example, have lower LAI and higher albedo (e.g. Bright et al., 2013). A constantly thinned age-less forest will therefore always lead to a lower albedo than a young forest regrowing after a clear-cut.

3.3 Limitations and alternative schemes

In the previous sections we compared a JSBACH4–FF simulation when only using PFTs with simulations including forest age-classes and discussed associated trade-offs and benefits. In this section we discuss limitations and advantages of the applied and of alternative schemes.

Since JSBACH is a tile-based DGVM, the introduction of an individual/cohort-based approach as used in some other DGVMs (e.g. Sato et al., 2007; Fisher et al., 2015; Bayer et al., 2017) would be very complex. Regarding forest age-structures these models have the essential advantage of naturally providing forest demography (Fisher et al., 2018). Due to their complexity, however, they are less commonly used as fully coupled LSMs for ESMs. Being fully coupled with an ESM, however, is one major aspect and purpose of JSBACH, which historically has been part of the MPI-ESM (Mauritsen et al., 2019) and now also is part of the ICON-ESM (Giorgetta et al., 2018).

For tile-based DGVMs, there is at least one option mentioned in the literature that provides an alternative to simply increasing the number of tiles: the coupling of a separated module dealing with the woody demography (see e.g. Bellassen et al., 2010; Haverd et al., 2018). On one hand, this approach shares the advantage with individual/cohort-based DGVMs that it provides a forest demography and thus principally enables the tracking of forest age. On the other hand, this approach has the important limitation of still calculating key ~~processes concerning the land–atmosphere coupling~~ land surface processes at the aggregated tile level, i.e. in this approach, processes such as photosynthesis and respiration, are not computed for separate age-classes. This restriction impairs the calculation of biogeochemical and biophysical interactions, due to the non-linearity of forest growth

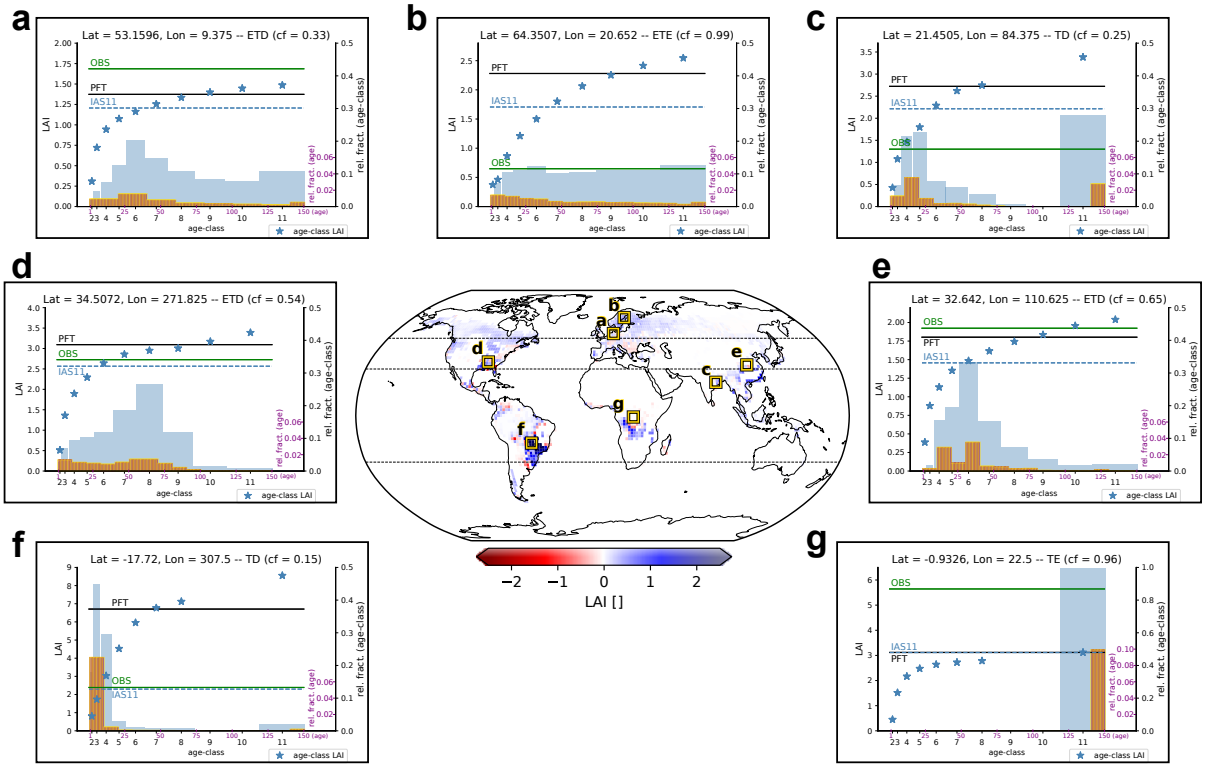

~~Exemplary~~

Figure 7. Example grid-points comparing ~~results of a simulation using age-classes to those of a PFT simulation and to the observation-based data. Shown are~~ 2001-2010 mean ~~summer gross primary production~~ spring leaf area index (~~JJA GPP~~MAM LAI) from ~~observation-based data compared to the JJA GPP resulting in two different simulations~~ the simulations without (PFT) and with age-classes (IAS11) to observation-based data. The map in the center shows the difference ~~between the absolute differences~~ of differences between the observation-based ~~JJA GPP per forested area~~ data and ~~those of~~ the simulations (abs(OBS-PFT)-abs(OBS-IAS11)), i.e. it shows where the results from the simulation with age-classes (IAS11) deviate less (blue) or more (red) from the observation-based data than the PFT simulation results (see also Figs. S4.2-S4.4, column 4). Dashed lines in the map mark the three selected regions ~~– boreal, northern hemisphere temperate, and tropical~~ (see Table 2). The plots (a-g) show the ~~JJA GPP per PFT area~~ LAI of selected PFTs (ETD: extratropical deciduous; ETE: extratropical evergreen; TD: tropical deciduous; TE: tropical evergreen) ~~and the~~ as well as their according area fractions per age-class and per year at the ~~different~~ labelled grid-points~~framed on the map~~. ~~For each grid-point the center~~ Center latitude~~and longitude~~, ~~as well as the~~ longitude and grid-cell cover fraction (cf) of the depicted PFT are ~~specified~~indicated. The x-axis reflects the age from 0-151 (purple) with the age-classes (black) indicated at the age centres. The ~~left y-axis depicts the amount of JJA GPP. Stars mark the JJA GPP per age-class, the dashed blue line the resulting JJA GPP value of the plotted PFT in the IAS11 simulation. The black line marks the JJA GPP value resulting from the PFT simulation, i.e. the simulation without age-classes. The green line marks the 2010 JJA GPP value from the observation-based data. The~~ two right y-axes represent the bars: depicted are the 2010 area fractions ~~per age-class (black) and per year (purple)~~ relative to the ~~plotted~~ area of the depicted PFT. Blue bars are per age-class (black y-axes) and depict the fraction of each age-class (i.e. one ~~separate~~ bar per age-class)~~and~~ ; the yellow framed purple bars depict the fraction of each age (i.e. one ~~separate~~ bar per year). The left y-axis depicts the LAI. Stars mark the simulated LAI per age-class, and the lines the LAI of the depicted PFT – blue dashed line: IAS11 simulation, black line: PFT simulation, green line: 2010 value from the observation-based data. Note: 1. The age-class ~~JJA GPP~~ LAI is only depicted for age-classes having non-zero fractional cover over the whole timespan 2001-2010 (this is not the case for the age-classes 9 and 10 in panel c, f and g). 2. Age and age-class fractions of classes 2-8 in panel g are very small and therefore not visible above the x-axis. 3. Since we did not apply any harvest in the final simulation year 2010, the first year and accordingly the youngest age-class are always empty.

and the associated non-linear relationships of those key processes with forest age (as e.g. depicted for ~~JJA GPP~~ spring LAI in Fig. 7). This limitation can only be avoided by increasing the number of tiles.

Building on the approach of increasing the number of tiles, the scheme suggested in this paper adds ~~one~~ an important benefit of the alternative schemes by explicitly tracking forest age. It thereby enables the implementation of age-based forest management schemes that historically were common in temperate forests and are still the dominant management type in boreal forests (Kuusela, 1994; Pan et al., 2011; Puettmann et al., 2015; Kuuluvainen and Gauthier, 2018). Another advantage of the explicit tracking concerns the discretisation error. While the presented approach does require frequent area-weighted merges in order to maintain a limited number of age-classes, it only requires to shift the actually affected parts of an age-class, and not entire age-classes/"cohorts" as common in previous applications (e.g. Shevliakova et al., 2009; Yue et al., 2018b). Upon ageing, for example, in our approach only those fractions of an age-class will be shifted that are actually at the age-limits of an age-class. An important restriction of the approach presented in this paper is that it is only applicable for a DGVM with a tile-hierarchy and would not be applicable for a DGVM with a flat tile-organisation, such as JSBACH3, since the different layers of the tile-hierarchy are used to introduce different processes. In a DGVM with a flat tile-organisation, the PFT level associated with the age-classes on the leaf level of the tile-hierarchy would be missing, which we use for the management of the forest age-classes and for the tracking of the exact forest age.

With regard to previous studies that increased the number of tiles in order to introduce a more detailed representation of the forest state, our evaluation indicates that the number of additional tiles used in previous applications might have been too ~~coarse~~few. Solely separating primary and secondary forests (e.g. Yang et al., 2010; Stocker et al., 2014a, b) or introducing only a few age-classes/"cohorts" (e.g. Shevliakova et al., 2009; Yue et al., 2018b) might not be sufficient to discretise non-linear relationships with forest age (see e.g. Fig. 7, and also Fig. 6), at least not on the coarse resolutions that are common in global model studies dealing with human land use (e.g. Le Quéré et al., 2018).

In this paper, we presented two different approaches to distribute the age space onto the available age-classes: the equal age distribution scheme EAS, which spreads the age-classes evenly, and IAS, a scheme that increases the age space with increasing age. The evaluation indicated the second approach to be superior to the first (Fig. 6), which can be explained by the finer discretisation of younger age-classes that more accurately resolves the steep part of the non-linear age-dependent relationship of GPP, LAI and AGB (see e.g. Fig. 7). There are, however, other possible age distribution schemes. One could, for example, use smaller age-classes for old ages in addition to the smaller age-classes used for young ages in the IAS scheme. With such a scheme, one could better cover age-related declines as indicated in Fig. 7b or described in Zaehle et al. (2006) and Bellassen et al. (2010). Another possibility would be to replace the static distribution schemes that are equally applied to all grid-cells with a dynamic scheme creating individual distributions for each grid-cell. In such a dynamic scheme, age-classes could be defined depending on the demand for each grid-cell, with merging based on similarity criteria (see e.g. Shevliakova et al., 2009), i.e. ~~those~~ age-classes ~~would be merged that share the most~~ sharing similar values for a selected variable (e.g. GPP) could be merged creating space for new age-classes covering an age-space with less similar values. Such an approach could potentially further decrease the discretisation error, particularly for cells with only infrequent disturbances/harvest events. A drawback could be an increase in the organisational overhead caused by the similarity tests required for each merging step. However, the

additional computational effort is not expected to be very large, considering that ~~for now~~ currently the organisational overhead seems to be very small (~~linear increase without an~~ no striking offset as shown in Fig. 6d) and particularly since in the current set-up dynamic merges would only be required once a year.

4 Summary and Outlook

In this paper we described a new scheme to introduce forest age-structure in a hierarchical tile-based DGVM and presented its implementation in JSBACH4. JSBACH4–FF allows ~~land–atmosphere interactions~~ key land surface processes to be simulated in dependence of forest age and, simultaneously, to trace the exact forest age, ~~enabling the~~ which is a precondition for any implementation of age-based forest management schemes in JSBACH4–FF.

JSBACH4 itself is still highly under development regarding infrastructure and processes integrated from JSBACH3. In the version used for this paper (4.20p7), particularly the representation of natural and anthropogenic land cover change has not yet been ported from JSBACH3. Upon implementation, new processes will have to be integrated with the age structure. In addition, other developments would be desirable: harvest, for example, has so far only been implemented as area clear cuts, following the implementation of other disturbances in JSBACH3 (see Brovkin et al., 2009). For a representation of different forest management strategies including intermediate thinning before a final felling, an implementation of forest thinning would be required (Otto et al., 2014; Naudts et al., 2015). Anthropogenic thinning could be implemented in JSBACH4–FF by keeping the number of individuals as a state variable for each age-class that is manipulated upon thinning, with anthropogenic thinning overruling the already implemented self-thinning.

Despite planned and potential extensions, together with the newly implemented age-classes, JSBACH4–FF already now provides a valuable tool to study forest management effects, particularly due to its integration with the ICON-ESM.

Code and data availability. The hosting MPI-ESM model version (MPI-ESM 1.2.01p1) is made available under a version of the MPI-M Software License Agreement and can be obtained after registration from https://www.mpimet.mpg.de/en/science/models/mpi-esm/users-forum/. Data and scripts used in the analysis, the JSBACH4 (4.20p7; git feature/forests) code, a patch to the hosting MPI-ESM required to run JSBACH4–FF as well as other supplementary informations are archived by the Max Planck Institute for Meteorology (https://pure.mpg.de/pubman/faces/ViewItemFullPage.jsp?itemId=item_3032727) and can be obtained by contacting publications@mpimet.mpg.de.

Author contributions. JN, KN and JP initiated the implementation of age-classes in JSBACH. JN planned and conducted the implementation, designed and performed the simulations and wrote the first draft of the paper. All co-authors contributed to the analysis and edited the manuscript.

Acknowledgements. This work has been supported by the German Research Foundation's Emmy Noether Program (PO1751/1-1). All simulations have been conducted at the German Climate Computing Center (DKRZ; allocation bm0891). The authors like to thank Stiig Wilkenskjeld for reviewing the manuscript prior submission, Veronika Gayler for support regarding JSBACH3, Reiner Schnur for support regarding JSBACH4, and Thomas Raddatz for discussions regarding the implementation of the age-classes.

References

Amiro, B., Orchansky, A., Barr, A., Black, T., Chambers, S., III, F. C., Goulden, M., Litvak, M., Liu, H., McCaughey, J., McMillan, A., and Randerson, J.: The effect of post-fire stand age on the boreal forest energy balance, Agricultural and Forest Meteorology, 140, 41–50, https://doi.org/10.1016/j.agrformet.2006.02.014, the Fluxnet-Canada Research Network: Influence of Climate and Disturbance on Carbon Cycling in Forests and Peatlands, 2006.

Avitabile, V., Herold, M., Heuvelink, G. B. M., Lewis, S. L., Phillips, O. L., Asner, G. P., Armston, J., Ashton, P. S., Banin, L., Bayol, N., Berry, N. J., Boeckx, P., de Jong, B. H. J., DeVries, B., Girardin, C. A. J., Kearsley, E., Lindsell, J. A., Lopez-Gonzalez, G., Lucas, R., Malhi, Y., Morel, A., Mitchard, E. T. A., Nagy, L., Qie, L., Quinones, M. J., Ryan, C. M., Ferry, S. J. W., Sunderland, T., Laurin, G. V., Gatti, R. C., Valentini, R., Verbeeck, H., Wijaya, A., and Willcock, S.: An integrated pan-tropical biomass map using multiple reference datasets, Global Change Biology, 22, 1406–1420, https://doi.org/10.1111/gcb.13139, 2016.

Bayer, A. D., Lindeskog, M., Pugh, T. A. M., Anthoni, P. M., Fuchs, R., and Arneth, A.: Uncertainties in the land-use flux resulting from land-use change reconstructions and gross land transitions, Earth System Dynamics, 8, 91–111, https://doi.org/10.5194/esd-8-91-2017, 2017.

Bellassen, V., Maire, G. L., Dhôte, J., Ciais, P., and Viovy, N.: Modelling forest management within a global vegetation model—Part 1: Model structure and general behaviour, Ecological Modelling, 221, 2458–2474, https://doi.org/10.1016/j.ecolmodel.2010.07.008, 2010.

Besnard, S., Carvalhais, N., Arain, M. A., Black, A., de Bruin, S., Buchmann, N., Cescatti, A., Chen, J., Clevers, J. G. P. W., Desai, A. R., Gough, C. M., Havrankova, K., Herold, M., Hörtnagl, L., Jung, M., Knohl, A., Kruijt, B., Krupkova, L., Law, B. E., Lindroth, A., Noormets, A., Roupsard, O., Steinbrecher, R., Varlagin, A., Vincke, C., and Reichstein, M.: Quantifying the effect of forest age in annual net forest carbon balance, Environmental Research Letters, 13, 124 018, https://doi.org/10.1088/1748-9326/aaeaeb, https://doi.org/10.1088%2F1748-9326%2Faaeaeb, 2018.

Boserup, E.: The conditions of agricultural growth: the economics of agrarian change under population pressure., vol. 4, Earthscan, London, 1966.

Bright, R. M., Astrup, R., and Strømman, A. H.: Empirical models of monthly and annual albedo in managed boreal forests of interior Norway, Climatic Change, 120, 183–196, https://doi.org/10.1007/s10584-013-0789-1, 2013.

Brovkin, V., Raddatz, T., Reick, C. H., Claussen, M., and Gayler, V.: Global biogeophysical interactions between forest and climate, Geophysical Research Letters, 36, https://doi.org/10.1029/2009GL037543, 2009.

Dore, S., Kolb, T. E., Montes-Helu, M., Eckert, S. E., Sullivan, B. W., Hungate, B. A., Kaye, J. P., Hart, S. C., Koch, G. W., and Finkral, A.: Carbon and water fluxes from ponderosa pine forests disturbed by wildfire and thinning, Ecological Applications, 20, 663–683, https://doi.org/10.1890/09-0934.1, 2010.

Erb, K.-H., Luyssaert, S., Meyfroidt, P., Pongratz, J., Don, A., Kloster, S., Kuemmerle, T., Fetzel, T., Fuchs, R., Herold, M., Haberl, H., Jones, C. D., Marín-Spiotta, E., McCallum, I., Robertson, E., Seufert, V., Fritz, S., Valade, A., Wiltshire, A., and Dolman, A. J.: Land management: data availability and process understanding for global change studies, Global Change Biology, 23, 512–533, https://doi.org/10.1111/gcb.13443, 2017.

Fisher, R. A., Muszala, S., Verteinstein, M., Lawrence, P., Xu, C., McDowell, N. G., Knox, R. G., Koven, C., Holm, J., Rogers, B. M., Spessa, A., Lawrence, D., and Bonan, G.: Taking off the training wheels: the properties of a dynamic vegetation model without climate envelopes, CLM4.5(ED), Geoscientific Model Development, 8, 3593–3619, https://doi.org/10.5194/gmd-8-3593-2015, 2015.

Fisher, R. A., Koven, C. D., Anderegg, W. R. L., Christoffersen, B. O., Dietze, M. C., Farrior, C. E., Holm, J. A., Hurtt, G. C., Knox, R. G., Lawrence, P. J., Lichstein, J. W., Longo, M., Matheny, A. M., Medvigy, D., Muller-Landau, H. C., Powell, T. L., Serbin, S. P., Sato, H., Shuman, J. K., Smith, B., Trugman, A. T., Viskari, T., Verbeeck, H., Weng, E., Xu, C., Xu, X., Zhang, T., and Moorcroft, P. R.: Vegetation demographics in Earth System Models: A review of progress and priorities, Global Change Biology, 24, 35–54, https://doi.org/10.1111/gcb.13910, 2018.

Giorgetta, M. A., Brokopf, R., Crueger, T., Esch, M., Fiedler, S., Helmert, J., Hohenegger, C., Kornblueh, L., Köhler, M., Manzini, E., Mauritsen, T., Nam, C., Raddatz, T., Rast, S., Reinert, D., Sakradzija, M., Schmidt, H., Schneck, R., Schnur, R., Silvers, L., Wan, H., Zängl, G., and Stevens, B.: ICON-A, the Atmosphere Component of the ICON Earth System Model: I. Model Description, Journal of Advances in Modeling Earth Systems, 10, 1613–1637, https://doi.org/10.1029/2017MS001242, 2018.

Haverd, V., Smith, B., Nieradzik, L. P., and Briggs, P. R.: A stand-alone tree demography and landscape structure module for Earth system models: integration with inventory data from temperate and boreal forests, Biogeosciences, 11, 4039–4055, https://doi.org/10.5194/bg-11-4039-2014, 2014.

Haverd, V., Smith, B., Nieradzik, L., Briggs, P. R., Woodgate, W., Trudinger, C. M., Canadell, J. G., and Cuntz, M.: A new version of the CABLE land surface model (Subversion revision r4601) incorporating land use and land cover change, woody vegetation demography, and a novel optimisation-based approach to plant coordination of photosynthesis, Geoscientific Model Development, 11, 2995–3026, https://doi.org/10.5194/gmd-11-2995-2018, 2018.

Hurtt, G. C., Chini, L. P., Frolking, S., Betts, R. A., Feddema, J., Fischer, G., Fisk, J. P., Hibbard, K., Houghton, R. A., Janetos, A., Jones, C. D., Kindermann, G., Kinoshita, T., Klein Goldewijk, K., Riahi, K., Shevliakova, E., Smith, S., Stehfest, E., Thomson, A., Thornton, P., van Vuuren, D. P., and Wang, Y. P.: Harmonization of land-use scenarios for the period 1500–2100: 600 years of global gridded annual land-use transitions, wood harvest, and resulting secondary lands, Climatic Change, 109, 117, https://doi.org/10.1007/s10584-011-0153-2, 2011.

Juang, J.-Y., Katul, G., Siqueira, M., Stoy, P., and Novick, K.: Separating the effects of albedo from eco-physiological changes on surface temperature along a successional chronosequence in the southeastern United States, Geophysical Research Letters, 34, https://doi.org/10.1029/2007GL031296, 2007.

Kim, H., Yoshimura, K., Chang, E., Famiglietti, J. S., and Oki, T.: Century long observation constrained global dynamic downscaling and hydrologic implication, AGU Fall Meeting Abstracts, GC31D-02, 2012.

Kirschbaum, M. U. F., Whitehead, D., Dean, S. M., Beets, P. N., Shepherd, J. D., and Ausseil, A.-G. E.: Implications of albedo changes following afforestation on the benefits of forests as carbon sinks, Biogeosciences, 8, 3687–3696, https://doi.org/10.5194/bg-8-3687-2011, 2011.

Kondo, M., Ichii, K., Patra, P. K., Poulter, B., Calle, L., Koven, C., Pugh, T. A. M., Kato, E., Harper, A., Zaehle, S., and Wiltshire, A.: Plant Regrowth as a Driver of Recent Enhancement of Terrestrial CO2 Uptake, Geophysical Research Letters, 45, 4820–4830, https://doi.org/10.1029/2018GL077633, 2018.

Körner, C.: Plant CO2 responses: an issue of definition, time and resource supply, New Phytologist, 172, 393–411, https://doi.org/10.1111/j.1469-8137.2006.01886.x, 2006.

Krause, A., Pugh, T. A. M., Bayer, A. D., Li, W., Leung, F., Bondeau, A., Doelman, J. C., Humpenöder, F., Anthoni, P., Bodirsky, B. L., Ciais, P., Müller, C., Murray-Tortarolo, G., Olin, S., Popp, A., Sitch, S., Stehfest, E., and Arneth, A.: Large uncertainty in carbon uptake potential of land-based climate-change mitigation efforts, Global Change Biology, 24, 3025–3038, https://doi.org/10.1111/gcb.14144, 2018.

Kuuluvainen, T. and Gauthier, S.: Young and old forest in the boreal: critical stages of ecosystem dynamics and management under global change, Forest Ecosystems, 5, 26, https://doi.org/10.1186/s40663-018-0142-2, 2018.

Kuusela, K.: Forest resources in Europe 1950-1990, vol. 1, Cambridge University Press, 1994.

Lawrence, D. M., Hurtt, G. C., Arneth, A., Brovkin, V., Calvin, K. V., Jones, A. D., Jones, C. D., Lawrence, P. J., de Noblet-Ducoudré, N., Pongratz, J., Seneviratne, S. I., and Shevliakova, E.: The Land Use Model Intercomparison Project (LUMIP) contribution to CMIP6: rationale and experimental design, Geoscientific Model Development, 9, 2973–2998, https://doi.org/10.5194/gmd-9-2973-2016, 2016.

Le Quéré, C., Moriarty, R., Andrew, R. M., Canadell, J. G., Sitch, S., Korsbakken, J. I., Friedlingstein, P., Peters, G. P., Andres, R. J., Boden, T. A., Houghton, R. A., House, J. I., Keeling, R. F., Tans, P., Arneth, A., Bakker, D. C. E., Barbero, L., Bopp, L., Chang, J., Chevallier, F., Chini, L. P., Ciais, P., Fader, M., Feely, R. A., Gkritzalis, T., Harris, I., Hauck, J., Ilyina, T., Jain, A. K., Kato, E., Kitidis, V., Klein Goldewijk, K., Koven, C., Landschützer, P., Lauvset, S. K., Lefèvre, N., Lenton, A., Lima, I. D., Metzl, N., Millero, F., Munro, D. R., Murata, A., Nabel, J. E. M. S., Nakaoka, S., Nojiri, Y., O'Brien, K., Olsen, A., Ono, T., Pérez, F. F., Pfeil, B., Pierrot, D., Poulter, B., Rehder, G., Rödenbeck, C., Saito, S., Schuster, U., Schwinger, J., Séférian, R., Steinhoff, T., Stocker, B. D., Sutton, A. J., Takahashi, T., Tilbrook, B., van der Laan-Luijkx, I. T., van der Werf, G. R., van Heuven, S., Vandemark, D., Viovy, N., Wiltshire, A., Zaehle, S., and Zeng, N.: Global Carbon Budget 2015, Earth System Science Data, 7, 349–396, https://doi.org/10.5194/essd-7-349-2015, 2015.

Le Quéré, C., Andrew, R. M., Friedlingstein, P., Sitch, S., Pongratz, J., Manning, A. C., Korsbakken, J. I., Peters, G. P., Canadell, J. G., Jackson, R. B., Boden, T. A., Tans, P. P., Andrews, O. D., Arora, V. K., Bakker, D. C. E., Barbero, L., Becker, M., Betts, R. A., Bopp, L., Chevallier, F., Chini, L. P., Ciais, P., Cosca, C. E., Cross, J., Currie, K., Gasser, T., Harris, I., Hauck, J., Haverd, V., Houghton, R. A., Hunt, C. W., Hurtt, G., Ilyina, T., Jain, A. K., Kato, E., Kautz, M., Keeling, R. F., Klein Goldewijk, K., Körtzinger, A., Landschützer, P., Lefèvre, N., Lenton, A., Lienert, S., Lima, I., Lombardozzi, D., Metzl, N., Millero, F., Monteiro, P. M. S., Munro, D. R., Nabel, J. E. M. S., Nakaoka, S.-I., Nojiri, Y., Padin, X. A., Peregon, A., Pfeil, B., Pierrot, D., Poulter, B., Rehder, G., Reimer, J., Rödenbeck, C., Schwinger, J., Séférian, R., Skjelvan, I., Stocker, B. D., Tian, H., Tilbrook, B., Tubiello, F. N., van der Laan-Luijkx, I. T., van der Werf, G. R., van Heuven, S., Viovy, N., Vuichard, N., Walker, A. P., Watson, A. J., Wiltshire, A. J., Zaehle, S., and Zhu, D.: Global Carbon Budget 2017, Earth System Science Data, 10, 405–448, https://doi.org/10.5194/essd-10-405-2018, 2018.

Leslie, A., Mencuccini, M., and Perks, M.: Preliminary growth functions for Eucalyptus gunnii in the UK, Biomass and Bioenergy, 108, 464–469, https://doi.org/10.1016/j.biombioe.2017.10.037, 2018.

Luyssaert, S., Jammet, M., Stoy, P. C., Estel, S., Pongratz, J., Ceschia, E., Churkina, G., Don, A., Erb, K., Ferlicoq, M., et al.: Land management and land-cover change have impacts of similar magnitude on surface temperature, Nature Climate Change, 4, 389, 2014.

Martínez-Vilalta, J., Vanderklein, D., and Mencuccini, M.: Tree height and age-related decline in growth in Scots pine (Pinus sylvestris L.), Oecologia, 150, 529–544, https://doi.org/10.1007/s00442-006-0552-7, 2007.

Mauritsen, T., Bader, J., Becker, T., Behrens, J., Bittner, M., Brokopf, R., Brovkin, V., Claussen, M., Crueger, T., Esch, M., Fast, I., Fiedler, S., Fläschner, D., Gayler, V., Giorgetta, M., Goll, D. S., Haak, H., Hagemann, S., Hedemann, C., Hohenegger, C., Ilyina, T., Jahns, T., Jimenez de la Cuesta Otero, D., Jungclaus, J., Kleinen, T., Kloster, S., Kracher, D., Kinne, S., Kleberg, D., Lasslop, G., Kornblueh, L., Marotzke, J., Matei, D., Meraner, K., Mikolajewicz, U., Modali, K., Möbis, B., Müller, W. A., Nabel, J. E. M. S., Nam, C. C. W., Notz, D., Nyawira, S.-S., Paulsen, H., Peters, K., Pincus, R., Pohlmann, H., Pongratz, J., Popp, M., Raddatz, T., Rast, S., Redler, R., Reick, C. H., Rohrschneider, T., Schemann, V., Schmidt, H., Schnur, R., Schulzweida, U., Six, K. D., Stein, L., Stemmler, I., Stevens, B., von Storch, J.-S., Tian, F., Voigt, A., de Vrese, P., Wieners, K.-H., Wilkenskjeld, S., Winkler, A., and Roeckner, E.: Developments in the MPI-M Earth System Model version 1.2 (MPI-ESM 1.2) and its response to increasing CO2, Journal of Advances in Modeling Earth Systems, 0, https://doi.org/10.1029/2018MS001400, 2019.

Meinshausen, M., Vogel, E., Nauels, A., Lorbacher, K., Meinshausen, N., Etheridge, D. M., Fraser, P. J., Montzka, S. A., Rayner, P. J., Trudinger, C. M., Krummel, P. B., Beyerle, U., Canadell, J. G., Daniel, J. S., Enting, I. G., Law, R. M., Lunder, C. R., O'Doherty, S., Prinn, R. G., Reimann, S., Rubino, M., Velders, G. J. M., Vollmer, M. K., Wang, R. H. J., and Weiss, R.: Historical greenhouse gas concentrations for climate modelling (CMIP6), Geoscientific Model Development, 10, 2057–2116, https://doi.org/10.5194/gmd-10-2057-2017, 2017.

Melton, J. R. and Arora, V. K.: Competition between plant functional types in the Canadian Terrestrial Ecosystem Model (CTEM) v. 2.0, Geoscientific Model Development, 9, 323–361, https://doi.org/10.5194/gmd-9-323-2016, 2016.

Myneni, R., Hoffman, S., Knyazikhin, Y., Privette, J., Glassy, J., Tian, Y., Wang, Y., Song, X., Zhang, Y., Smith, G., Lotsch, A., Friedl, M., Morisette, J., Votava, P., Nemani, R., and Running, S.: Global products of vegetation leaf area and fraction absorbed PAR from year one of MODIS data, Remote Sensing of Environment, 83, 214–231, https://doi.org/10.1016/S0034-4257(02)00074-3, http://www.sciencedirect.com/science/article/pii/S0034425702000743, the Moderate Resolution Imaging Spectroradiometer (MODIS): a new generation of Land Surface Monitoring, 2002.

Nabel, J. E. M. S.: Upscaling with the dynamic two-layer classification concept (D2C): TreeMig-2L, an efficient implementation of the forest-landscape model TreeMig, Geoscientific Model Development, 8, 3563–3577, https://doi.org/10.5194/gmd-8-3563-2015, 2015.

Naudts, K., Ryder, J., McGrath, M. J., Otto, J., Chen, Y., Valade, A., Bellasen, V., Berhongaray, G., Bönisch, G., Campioli, M., Ghattas, J., De Groote, T., Haverd, V., Kattge, J., MacBean, N., Maignan, F., Merilä, P., Penuelas, J., Peylin, P., Pinty, B., Pretzsch, H., Schulze, E. D., Solyga, D., Vuichard, N., Yan, Y., and Luyssaert, S.: A vertically discretised canopy description for ORCHIDEE (SVN r2290) and the modifications to the energy, water and carbon fluxes, Geoscientific Model Development, 8, 2035–2065, https://doi.org/10.5194/gmd-8-2035-2015, 2015.

Naudts, K., Nabel, J. E. M. S., Sabot, M., and Pongratz, J.: Impact of age-dependent wood harvest on land surface properties, in prep.

Nyawira, S. S., Nabel, J. E. M. S., Don, A., Brovkin, V., and Pongratz, J.: Soil carbon response to land-use change: evaluation of a global vegetation model using observational meta-analyses, Biogeosciences, 13, 5661–5675, https://doi.org/10.5194/bg-13-5661-2016, 2016.

Otto, J., Berveiller, D., Bréon, F.-M., Delpierre, N., Geppert, G., Granier, A., Jans, W., Knohl, A., Kuusk, A., Longdoz, B., Moors, E., Mund, M., Pinty, B., Schelhaas, M.-J., and Luyssaert, S.: Forest summer albedo is sensitive to species and thinning: how should we account for this in Earth system models?, Biogeosciences, 11, 2411–2427, https://doi.org/10.5194/bg-11-2411-2014, 2014.

Pan, Y., Chen, J. M., Birdsey, R., McCullough, K., He, L., and Deng, F.: Age structure and disturbance legacy of North American forests, Biogeosciences, 8, 715–732, https://doi.org/10.5194/bg-8-715-2011, 2011.

Pan, Y., Birdsey, R. A., Phillips, O. L., and Jackson, R. B.: The Structure, Distribution, and Biomass of the World's Forests, Annual Review of Ecology, Evolution, and Systematics, 44, 593–622, https://doi.org/10.1146/annurev-ecolsys-110512-135914, 2013.

Pongratz, J., Reick, C., Raddatz, T., and Claussen, M.: A reconstruction of global agricultural areas and land cover for the last millennium, Global Biogeochemical Cycles, 22, https://doi.org/10.1029/2007GB003153, 2008.

Pongratz, J., Dolman, H., Don, A., Erb, K.-H., Fuchs, R., Herold, M., Jones, C., Kuemmerle, T., Luyssaert, S., Meyfroidt, P., and Naudts, K.: Models meet data: Challenges and opportunities in implementing land management in Earth system models, Global Change Biology, 24, 1470–1487, https://doi.org/10.1111/gcb.13988, 2017.

Poorter, L., Bongers, F., Aide, T. M., Almeyda Zambrano, A. M., Balvanera, P., Becknell, J. M., Boukili, V., Brancalion, P. H. S., Broadbent, E. N., Chazdon, R. L., Craven, D., de Almeida-Cortez, J. S., Cabral, G. A. L., de Jong, B. H. J., Denslow, J. S., Dent, D. H., DeWalt, S. J., Dupuy, J. M., Durán, S. M., Espírito-Santo, M. M., Fandino, M. C., César, R. G., Hall, J. S., Hernandez-Stefanoni, J. L., Jakovac, C. C., Junqueira, A. B., Kennard, D., Letcher, S. G., Licona, J.-C., Lohbeck, M., Marín-Spiotta, E., Martínez-Ramos, M., Massoca, P., Meave,

J. A., Mesquita, R., Mora, F., Muñoz, R., Muscarella, R., Nunes, Y. R. F., Ochoa-Gaona, S., de Oliveira, A. A., Orihuela-Belmonte, E., Peña-Claros, M., Pérez-García, E. A., Piotto, D., Powers, J. S., Rodríguez-Velázquez, J., Romero-Pérez, I. E., Ruíz, J., Saldarriaga, J. G., Sanchez-Azofeifa, A., Schwartz, N. B., Steininger, M. K., Swenson, N. G., Toledo, M., Uriarte, M., van Breugel, M., van der Wal, H., Veloso, M. D. M., Vester, H. F. M., Vicentini, A., Vieira, I. C. G., Bentos, T. V., Williamson, G. B., and Rozendaal, D. M. A.: Biomass resilience of Neotropical secondary forests, Nature, 530, 211, https://doi.org/10.1038/nature16512, 2016.

Poulter, B., Aragão, L., Andela, N., Bellassen, V., Ciais, P., Kato, T., Lin, X., Nachin, B., Luyssaert, S., Pederson, N., Peylin, P., Piao, S., Saatchi, S., Schepaschenko, D., Schelhaas, M., and Shivdenko, A.: The global forest age dataset (GFADv1.0), link to NetCDF file, https://doi.org/10.1594/PANGAEA.889943, 2018.

Puettmann, K. J., Wilson, S. M., Baker, S. C., Donoso, P. J., Drössler, L., Amente, G., Harvey, B. D., Knoke, T., Lu, Y., Nocentini, S., Putz, F. E., Yoshida, T., and Bauhus, J.: Silvicultural alternatives to conventional even-aged forest management - what limits global adoption?, Forest Ecosystems, 2, 8, https://doi.org/10.1186/s40663-015-0031-x, 2015.

Reick, C. H., Raddatz, T., Brovkin, V., and Gayler, V.: Representation of natural and anthropogenic land cover change in MPI-ESM, Journal of Advances in Modeling Earth Systems, 5, 459–482, https://doi.org/10.1002/jame.20022, 2013.

Sato, H., Itoh, A., and Kohyama, T.: SEIB–DGVM: A new Dynamic Global Vegetation Model using a spatially explicit individual-based approach, Ecological Modelling, 200, 279–307, https://doi.org/10.1016/j.ecolmodel.2006.09.006, 2007.

Shevliakova, E., Pacala, S. W., Malyshev, S., Hurtt, G. C., Milly, P. C. D., Caspersen, J. P., Sentman, L. T., Fisk, J. P., Wirth, C., and Crevoisier, C.: Carbon cycling under 300 years of land use change: Importance of the secondary vegetation sink, Global Biogeochemical Cycles, 23, https://doi.org/10.1029/2007GB003176, 2009.

Smith, B., Prentice, I. C., and Sykes, M. T.: Representation of vegetation dynamics in the modelling of terrestrial ecosystems: comparing two contrasting approaches within European climate space, Global Ecology and Biogeography, 10, 621–637, https://doi.org/10.1046/j.1466-822X.2001.t01-1-00256.x, 2001.

Soja, A. J., Shugart, H. H., Sukhinin, A., Conard, S., and Stackhouse, P. W.: Satellite-Derived Mean Fire Return Intervals As Indicators Of Change In Siberia (1995–2002), Mitigation and Adaptation Strategies for Global Change, 11, 75–96, https://doi.org/10.1007/s11027-006-1009-3, 2006.

Stocker, B. D., Feissli, F., Strassmann, K. M., Spahni, R., and Joos, F.: Past and future carbon fluxes from land use change, shifting cultivation and wood harvest, Tellus B: Chemical and Physical Meteorology, 66, 23 188, https://doi.org/10.3402/tellusb.v66.23188, 2014a.

Stocker, B. D., Spahni, R., and Joos, F.: DYPTOP: a cost-efficient TOPMODEL implementation to simulate sub-grid spatio-temporal dynamics of global wetlands and peatlands, Geoscientific Model Development, 7, 3089–3110, https://doi.org/10.5194/gmd-7-3089-2014, 2014b.

Sun, G., Noormets, A., Gavazzi, M., McNulty, S., Chen, J., Domec, J.-C., King, J., Amatya, D., and Skaggs, R.: Energy and water balance of two contrasting loblolly pine plantations on the lower coastal plain of North Carolina, USA, Forest Ecology and Management, 259, 1299–1310, https://doi.org/10.1016/j.foreco.2009.09.016, 2010.

Tramontana, G., Jung, M., Schwalm, C. R., Ichii, K., Camps-Valls, G., Ráduly, B., Reichstein, M., Arain, M. A., Cescatti, A., Kiely, G., Merbold, L., Serrano-Ortiz, P., Sickert, S., Wolf, S., and Papale, D.: Predicting carbon dioxide and energy fluxes across global FLUXNET sites with regression algorithms, Biogeosciences, 13, 4291–4313, https://doi.org/10.5194/bg-13-4291-2016, 2016.

van Mantgem, P. J., Stephenson, N. L., Byrne, J. C., Daniels, L. D., Franklin, J. F., Fulé, P. Z., Harmon, M. E., Larson, A. J., Smith, J. M., Taylor, A. H., and Veblen, T. T.: Widespread Increase of Tree Mortality Rates in the Western United States, Science, 323, 521–524, https://doi.org/10.1126/science.1165000, 2009.

Yang, X., Richardson, T. K., and Jain, A. K.: Contributions of secondary forest and nitrogen dynamics to terrestrial carbon uptake, Biogeosciences, 7, 3041–3050, https://doi.org/10.5194/bg-7-3041-2010, 2010.

Yao, Y., Piao, S., and Wang, T.: Future biomass carbon sequestration capacity of Chinese forests, Science Bulletin, 63, 1108–1117, https://doi.org/10.1016/j.scib.2018.07.015, 2018.

Yue, C., Ciais, P., and Li, W.: Smaller global and regional carbon emissions from gross land use change when considering sub-grid secondary land cohorts in a global dynamic vegetation model, Biogeosciences, 15, 1185–1201, https://doi.org/10.5194/bg-15-1185-2018, 2018a.

Yue, C., Ciais, P., Luyssaert, S., Li, W., McGrath, M. J., Chang, J., and Peng, S.: Representing anthropogenic gross land use change, wood harvest, and forest age dynamics in a global vegetation model ORCHIDEE-MICT v8.4.2, Geoscientific Model Development, 11, 409–428, https://doi.org/10.5194/gmd-11-409-2018, 2018b.

Zaehle, S., Sitch, S., Prentice, I. C., Liski, J., Cramer, W., Erhard, M., Hickler, T., and Smith, B.: The importance of age-related decline in forest NPP for modeling regional carbon balances, Ecological Applications, 16, 1555–1574, 2006.